Int. J. Solids Structures, 1972, Vol. 8, pp. 149 to 192. Pergamon Press. Printed in Great Britain

THEORETICAL STUDY OF STRESS CONCENTRATIONS AT CIRCULAR HOLES AND INCLUSIONS IN STRAIN HARDENING MATERIALS†

WU-CHENG HUANG

Harvard University, Cambridge, Massachusetts

Abstract—Nonlinear boundary value problems of an infinite elastic–plastic plate with a circular hole subjected to pure tension and pure shear at infinity are solved by a method involving fourier series and finite difference. On the basis of these solutions, the validity of Neuber's relationship between the stress and strain concentration factors for the plane stress problems is examined and a generalized Stowell formula for the stress concentration factor is proposed for problems in which the applied loading may be pure shear as well as pure tension and, furthermore, other stress states. By the same method of solution, the stress distributions around a rigid circular cylindrical inclusion embedded in an infinite rigid–plastic matrix subjected to uniform transverse pure shear and tension are obtained.

1. INTRODUCTION

THEORETICAL studies of stress concentrations around structural discontinuities in an elastic material have been made for a wide variety of cases, but few corresponding studies for strain hardening materials have been made. A number of authors have considered one dimensional plastic problems, such as an infinite plate with a circular hole under uniform radial load [1–4] and a circular cylindrical inclusion embedded in an infinite matrix subjected to uniform transverse radial stress [5]. The only two dimensional strain-hardening problem (i.e. with stress varying in two space coordinates) which has been well investigated is an infinite plate with a circular hole under pure tension [6–8].

In the present study, three two dimensional problems are investigated. Due to its importance and for the sake of comparison with earlier work, the elastic–plastic plate in tension with a circular hole (see Fig. 1) is considered first and followed by the problem of an infinite plate with a circular hole subjected to pure shear at infinity (see Fig. 2). This latter problem is relevant to such engineering structures as a thin-walled hollow beam with a small circular hole under torsion and the web with holes in an I beam subjected to severe transverse shearing load. As a first attempt to understand the stress concentration around a fiber in a fibrous reinforced composite, analyses of the stress distribution around a rigid circular cylindrical inclusion in an infinite matrix subjected to uniform transverse pure shear and tension (see Figs. 3 and 4) are made. Here the study is restricted to a rigid–plastic matrix with a power law strain hardening material.

Stowell [9] presented an approximate formula

$$K = \frac{(\sigma_\theta)_{a,\pi/2}}{\sigma_\infty} = 1 + 2\frac{(E_s)_{a,\pi/2}}{(E_s)_\infty}$$

† This work was supported in part by the National Aeronautics and Space Administration under Grant NGL 22-007-012, and by the Division of Engineering and Applied Physics, Harvard University.

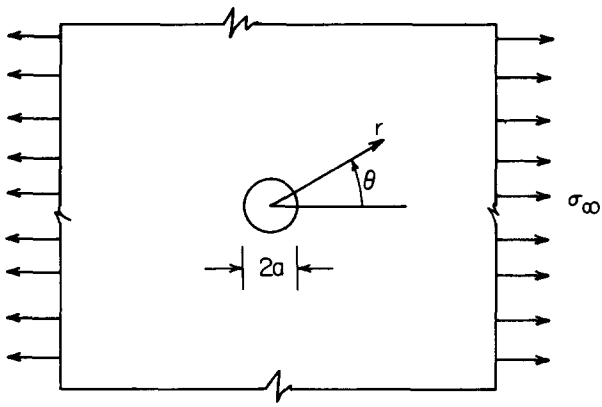

FIG. 1. Circular hole in an infinite plate subjected to pure tension.

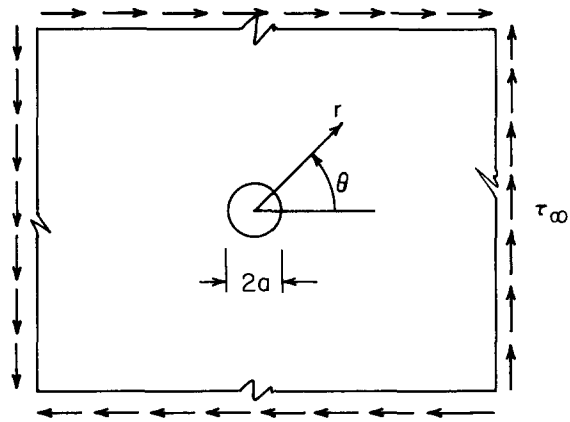

FIG. 2. Circular hole in an infinite plate subjected to pure shear.

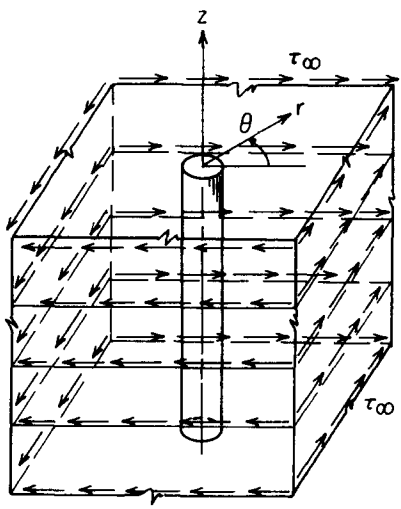

FIG. 3. Cylindrical inclusion in an infinite matrix subjected to transverse pure shear.

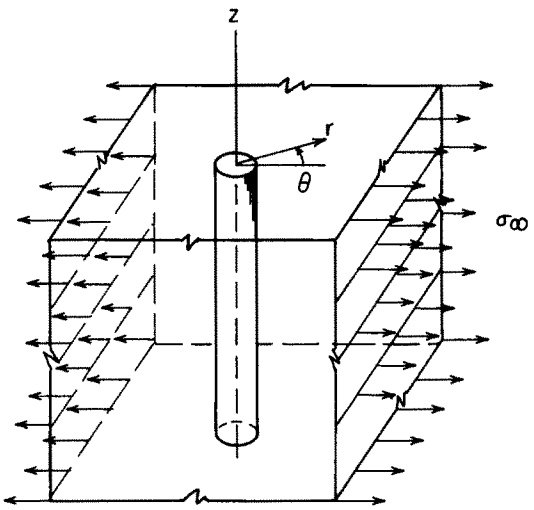

FIG. 4. Cylindrical inclusion in an infinite matrix subjected to transverse pure tension.

for the stress concentration factor K in a plate with a circular hole (see Fig. 1) subjected to pure tension; here E_s means the secant modulus. Based on experimental results, Hardrath and Ohman [10] generalized this formula for plates with arbitrary holes, notches and fillets under pure tension as

$$K_{\text{plastic}} = 1+(K_{\text{elastic}}-1)\frac{(E_s)_{\text{max stress}}}{(E_s)_\infty}.$$

Neuber [11] obtained a relationship between stress and strain concentration factors, namely,

$$K_\sigma K_\varepsilon = K_H^2$$

by considering a notched prismatic body under antiplane shear; here K_H is the elastic stress concentration factor. In the present study, based on the results of our analysis the validity of the Neuber rule for plane stress problems is examined and a generalized Stowell formula is proposed for problems in which the applied loading may be pure shear as well as pure tension and, furthermore, other stress states.

2. THE BOUNDARY VALUE PROBLEMS

Introduction

All the problems which are studied in this paper are concerned with two dimensional boundary value problems consisting of an infinite region exterior to a circular boundary. The ability to perform a plastic analysis of this kind of boundary value problem has been limited because of the uncertain stress–strain relation and the nonlinearity of the governing equation. The only stress–strain relations which have been used in the past to solve such problems are the simplest deformation theory of plasticity and the simplest incremental theory of plasticity. The use of a deformation theory in the solution of boundary value

problems requires much less work than the use of a corresponding incremental theory, but it has often been criticized on the grounds that deformation theories are physically unsound except for the case of proportional loading. It is shown in Ref. [12], however, that deformation theories of plasticity may be used for a range of loading paths other than proportional loading without violation of general requirements for the physical soundness of a plasticity theory.

In view of this, the J_2 deformation theory is employed in this analysis, and the acceptability can be justified by examination of the results by the criterion established in Ref. [12].

Because of the nonlinearity introduced by the constitutive equations of plasticity, finding the exact solution of boundary value problems is virtually hopeless, except for one dimensional problems. Approximate methods that have been employed are the Rayleigh–Ritz method [6], the finite element method [8] and the finite difference method [7]. In this section, a method involving fourier series and finite difference is presented. The governing equations, based on J_2 deformation theory and the Ramberg–Osgood stress–strain relation, are formulated in terms of a stress function for both plane stress and plane strain (under the restriction of no unloading). By taking advantage of the geometry, the solution is expanded into fourier series in the circumferential direction and the fourier coefficients, which are functions of the radial coordinate only, are determined by a finite difference method. Here the Potters' method [13] is employed.

Ramberg–Osgood uniaxial stress–strain relation

Ramberg and Osgood [14] suggested that the uniaxial stress–strain curve for a variety of structural materials can be described by the formula

$$\varepsilon = \frac{\sigma}{E}\left[1+\frac{3}{7}\left(\frac{\sigma}{\sigma_I}\right)^{n-1}\right] \tag{2.1}$$

where σ and ε are the uniaxial stress and strain, respectively. Here E is the elastic modulus, and n is a parameter chosen to provide the best fit to the stress–strain curve of a particular material under consideration. The nominal yield stress σ_I may be interpreted in either of two ways. It may be considered as an arbitrary parameter providing for a best fit or it is equal to the value of the stress at which the secant modulus E_s is equal to 0·7 E. Figure 5 shows plots of σ/σ_I vs. $E\varepsilon/\sigma_I$ for several values of n.

It may be noted that this relation gives the elastic relation $\varepsilon = \sigma/E$ for $\sigma \ll \sigma_I$ and gives the pure power law relation $\varepsilon = k\sigma^n$ for $\sigma \gg \sigma_I$.

J_2 deformation theory of plasticity

Based on the simplest total deformation theory of plasticity and the von Mises yield criterion, the strains are related to the stresses by

$$\varepsilon_{ij} = \frac{1+\nu}{E}\sigma_{ij} - \frac{\nu}{E}\delta_{ij}\sigma_{kk} + \frac{3}{2}\left(\frac{1}{E_s}-\frac{1}{E}\right)S_{ij} \tag{2.2}$$

where ν is the Poisson's ratio, E_s is the secant modulus of the uniaxial stress–strain curve at the effective stress given by

$$\hat{\sigma} = \sqrt{(\tfrac{3}{2}S_{ij}S_{ij})}$$

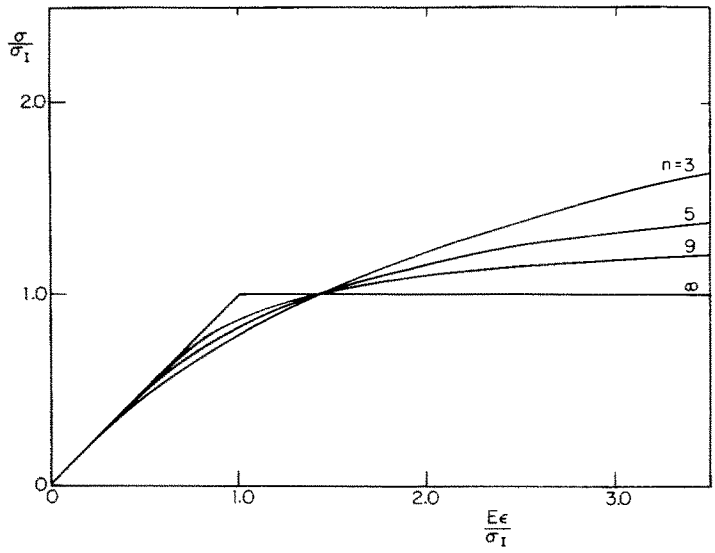

FIG. 5. Nondimensional Ramberg–Osgood stress–strain curves.

and S_{ij} is the stress deviator defined by

$$S_{ij} = \sigma_{ij} - \tfrac{1}{3}\sigma_{kk}\delta_{ij}.$$

Any solution must, of course, be checked to insure that $\hat{\sigma}$ at every point is non-decreasing (i.e. there must not be unloading). Furthermore, it is desirable to examine the extent of the deviation of the stress path at every point from proportional loading by the criterion of Ref. [12] in order to make sure that the use of deformation theory does not violate basic requirements of the theory of plasticity.

Governing equations

In either generalized plane stress or plane strain, equilibrium is insured for all stresses derived from a stress function ϕ by

$$\sigma_r = r^{-1}\phi' + r^{-2}\phi^{\cdot\cdot}, \qquad \sigma_\theta = \phi'', \qquad \sigma_{r\theta} = r^{-2}\phi^{\cdot} - r^{-1}\phi^{\cdot\prime}$$

where r, θ are cylindrical coordinates and $(\ )' = \partial/\partial r$, $(\ )^{\cdot} = \partial/\partial\theta$.

The strains must satisfy the compatibility equation

$$(r\varepsilon_\theta)'' + r^{-1}\varepsilon_r^{\cdot\cdot} - \varepsilon_r' - 2r^{-1}(\varepsilon_{r\theta}^{\cdot} r)' = 0.$$

In plane stress, the stress components acting on the plane parallel to the plate are neglected. The effective stress is therefore

$$\hat{\sigma}^2 = \sigma_r^2 + \sigma_\theta^2 - \sigma_r\sigma_\theta + 3\sigma_{r\theta}^2$$

while the strains are given, by (2.2), as

$$\varepsilon_r = \frac{1}{E}(\sigma_r - \nu\sigma_\theta) + \left(\frac{1}{E_s} - \frac{1}{E}\right)\left(\sigma_r - \frac{1}{2}\sigma_\theta\right)$$

$$\varepsilon_\theta = \frac{1}{E}(\sigma_\theta - \nu\sigma_r) + \left(\frac{1}{E_s} - \frac{1}{E}\right)\left(\sigma_\theta - \frac{1}{2}\sigma_r\right)$$

$$\varepsilon_{r\theta} = \frac{1+\nu}{E}\sigma_{r\theta} + \frac{3}{2}\left(\frac{1}{E_s} - \frac{1}{E}\right)\sigma_{r\theta}.$$

Here

$$\frac{1}{E_s} = \frac{1}{E}\left[1 + \frac{3}{7}\left(\frac{\hat{\sigma}}{\sigma_I}\right)^{n-1}\right],$$

if the Ramberg–Osgood formula is used.

With the introduction of the non-dimensional quantities

$$S_r = \frac{\sigma_r}{\sigma_\infty}, \qquad S_\theta = \frac{\sigma_\theta}{\sigma_\infty}, \qquad S_{r\theta} = \frac{\sigma_{r\theta}}{\sigma_\infty}, \qquad \hat{S} = \frac{\hat{\sigma}}{\sigma_\infty}$$

$$\lambda = \frac{\sigma_\infty}{\sigma_I}, \qquad p = \frac{3}{7}\lambda^{n-1}, \qquad x = \frac{a}{r}, \qquad F = x^2\frac{\phi}{\sigma_\infty}$$

the compatibility equation becomes

$$x^2\varepsilon_\theta'' + \varepsilon_r^{\cdot\cdot} + x\varepsilon_r' - 2\varepsilon_{r\theta}^{\cdot} + 2x\varepsilon_{r\theta}'^{\cdot} = 0 \tag{2.3}$$

where $(\,)' = \partial/\partial x$, $(\,)^{\cdot} = \partial/\partial\theta$, the stress components in terms of the modified stress function F are

$$\begin{aligned} S_r &= 2F - xF' + F^{\cdot\cdot} \\ S_\theta &= 2F - 2xF' + x^2F'' \\ S_{r\theta} &= xF'^{\cdot} - F^{\cdot} \end{aligned} \tag{2.4}$$

and the stress–strain relations are

$$\begin{aligned} \varepsilon_r &= \frac{\sigma_\infty}{E}(S_r - \nu S_\theta) + \sigma_\infty\left(\frac{1}{E_s} - \frac{1}{E}\right)\left(S_r - \frac{1}{2}S_\theta\right) \\ \varepsilon_\theta &= \frac{\sigma_\infty}{E}(S_\theta - \nu S_r) + \sigma_\infty\left(\frac{1}{E_s} - \frac{1}{E}\right)\left(S_\theta - \frac{1}{2}S_r\right) \\ \varepsilon_{r\theta} &= \frac{\sigma_\infty}{E}(1+\nu)S_{r\theta} + \frac{3}{2}\sigma_\infty\left(\frac{1}{E_s} - \frac{1}{E}\right)S_{r\theta} \end{aligned} \tag{2.5}$$

where

$$\frac{1}{E_s} = \frac{1}{E}(1 + p\hat{S}^{n-1}).$$

It may be noted that the infinite region exterior to the circular boundary has been transformed into a unit circle.

Substitution of equations (2.4), (2.5) into equation (2.3) gives the following governing equation in terms of the modified function F:

$$\begin{aligned}&(1+p\hat{S}^{n-1})(2x^4F''''+4x^3F'''-2x^2F''+4x^2F'''''+2xF'-4xF'''+8F'''+2F''''')\\&+p[(\hat{S}^{n-1})'(4x^4F'''+x^3F''-2x^2F'+4x^2F'''+2xF-4xF'')\\&+(\hat{S}^{n-1})'(4x^2F'''-6xF''+10F'+4F''')+6(\hat{S}^{n-1})''(x^2F''-xF')\\&+(\hat{S}^{n-1})''(2x^2F-3x^3F'+2x^4F''-x^2F'')+(\hat{S}^{n-1})'''(2F+2F''-x^2F'')]=0\end{aligned}\tag{2.6}$$

where

$$\hat{S}=(S_r^2+S_\theta^2-S_rS_\theta+3S_{r\theta}^2)^{\frac{1}{2}}.$$

For $p\to 0$ or $n=1$, this equation leads to the homogeneous linear partial differential equation

$$x^4F''''+2x^3F'''-x^2F''+2x^2F'''''+xF'-2xF'''+4F'''+F''''''=0\tag{2.7}$$

which is the governing equation for the elastic solution. On the other hand, for $p\to\infty$ equation (2.6) can be reduced to

$$\begin{aligned}&\tilde{S}^2(2x^4F''''+4x^3F'''-2x^2F''+4x^2F'''''+2xF'-4xF'''+8F'''+2F''''')\\&+\tfrac{1}{2}(n-1)[\tfrac{1}{2}(n-3)\tilde{S}'^2+\tilde{S}\tilde{S}''](2x^2F-3x^3F'+2x^4F''-x^2F'')\\&+\tfrac{1}{2}(n-1)\tilde{S}\tilde{S}'(4x^4F'''+x^3F''-2x^2F'+4x^2F'''+2xF-4xF'')\\&+\tfrac{1}{2}(n-1)\tilde{S}\tilde{S}'(4x^2F'''-6xF''+10F'+4F''')\\&+\tfrac{1}{2}(n-1)[\tfrac{1}{2}(n-3)\tilde{S}'^2+\tilde{S}\tilde{S}''](2F+2F''-x^2F'')\\&+\tfrac{1}{2}(n-1)[\tfrac{1}{2}(n-3)\tilde{S}'\tilde{S}'+\tilde{S}\tilde{S}''](6x^2F''-6xF')=0\end{aligned}\tag{2.8}$$

where $\tilde{S}=\hat{S}^2$. This is the governing equation for the problems in which the uniaxial stress–strain relation is taken to be a pure power law. It is worthy of note that the degree of the nonlinearity is independent of n.

In plane strain, if the strain component in the longitudinal direction is assumed to vanish (i.e. $\varepsilon_z=0$), the corresponding stress component can be expressed as

$$\sigma_z=\frac{1}{2}(\sigma_r+\sigma_\theta)+\left(\nu-\frac{1}{2}\right)\frac{E_s}{E}(\sigma_r+\sigma_\theta)$$

and the stress–strain relations are given by

$$\begin{aligned}\varepsilon_r&=\frac{1}{E}\left[\left(1-\frac{\nu}{2}\right)\sigma_r-\frac{3\nu}{2}\sigma_\theta\right]+\frac{3}{4}\left(\frac{1}{E_s}-\frac{1}{E}\right)(\sigma_r-\sigma_\theta)+\frac{E_s}{E}\left(\frac{1}{2}-\nu\right)\left[\frac{\nu}{E}+\frac{1}{2}\left(\frac{1}{E_s}-\frac{1}{E}\right)\right](\sigma_r+\sigma_\theta)\\\varepsilon_\theta&=\frac{1}{E}\left[\left(1-\frac{\nu}{2}\right)\sigma_\theta-\frac{3\nu}{2}\sigma_r\right]+\frac{3}{4}\left(\frac{1}{E_s}-\frac{1}{E}\right)(\sigma_\theta-\sigma_r)+\frac{E_s}{E}\left(\frac{1}{2}-\nu\right)\left[\frac{\nu}{E}+\frac{1}{2}\left(\frac{1}{E_s}-\frac{1}{E}\right)\right](\sigma_r+\sigma_\theta)\\\varepsilon_{r\theta}&=\frac{1+\nu}{E}\sigma_{r\theta}+\frac{3}{2}\left(\frac{1}{E_s}-\frac{1}{E}\right)\sigma_{r\theta}.\end{aligned}$$

By introducing the same non-dimensional quantities as in the plane stress case and with the use of the Ramberg–Osgood relation, we obtain the governing equation as

$$\left[1-\frac{\nu}{2}+\frac{3}{4}p\hat{S}^{n-1}+\frac{(\frac{1}{2}-\nu)(\nu+\frac{1}{2}p\hat{S}^{n-1})}{1+p\hat{S}^{n-1}}\right](x^4F''''+2x^3F'''+2x^2F'''''+xF'-x^2F''$$
$$-2xF'''+4F''+F'''')+\tfrac{3}{4}p[(\hat{S}^{n-1})'(2x^4F'''+x^3F''-x^2F'+2x^2F'''-3xF'')$$
$$+(\hat{S}^{n-1})'(2x^2F'''-2xF''+2F'''+4F')+(\hat{S}^{n-1})''(x^4F''-x^3F'-x^2F'')$$
$$+4(\hat{S}^{n-1})'(x^2F''-xF')+(\hat{S}^{n-1})''(F''+xF'-x^2F'')]$$
$$+\frac{p(\frac{1}{2}-\nu)^2}{(1+p\hat{S}^{n-1})^2}\Bigg[(\hat{S}^{n-1})'(2x^4F''''-x^3F''-x^2F'+2x^2F'''+4xF+xF'')$$
$$+2(\hat{S}^{n-1})'(4F'-3xF''+x^2F'''+F''')+\left\{(\hat{S}^{n-1})''-\frac{2p(\hat{S}^{n-1})'^2}{1+p\hat{S}^{n-1}}\right\}(4x^2F$$
$$-3x^3F'+x^4F''+x^2F'')+\left\{(\hat{S}^{n-1})''-\frac{2p(\hat{S}^{n-1})'^2}{1+p\hat{S}^{n-1}}\right\}(4F-3xF'+x^2F''+F'')\Bigg]=0 \qquad (2.9)$$

where the effective stress can be expressed in an implicit form as

$$\hat{S}^2=3\left[\left(\frac{S_r-S_\theta}{2}\right)^2+S_{r\theta}^2\right]+\left(\frac{\nu-\frac{1}{2}}{1+p\hat{S}^{n-1}}\right)^2(S_r+S_\theta)^2. \qquad (2.10)$$

For $p\to 0$ or $n=1$, this equation also provides equation (2.7), and for $p\to\infty$, it can be reduced to

$$\tilde{S}^2(x^4F''''+2x^3F'''-x^2F''+2x^2F'''''+xF'-2xF'''+4F''+F'''')$$
$$+\tfrac{1}{2}(n-1)[\tfrac{1}{2}(n-3)\tilde{S}'^2+\tilde{S}\tilde{S}''](x^4F''-x^3F'-x^2F'')$$
$$+\tfrac{1}{2}(n-1)\tilde{S}\tilde{S}'(2x^4F'''+x^3F''-x^2F'+2x^2F'''-3xF'')$$
$$+\tfrac{1}{2}(n-1)\tilde{S}\tilde{S}'(2x^2F'''-2xF''+2F'''+4F')$$
$$+\tfrac{1}{2}(n-1)[\tfrac{1}{2}(n-3)\tilde{S}'^2+\tilde{S}\tilde{S}'''](F''+xF'-x^2F'')$$
$$+\tfrac{1}{2}(n-1)[\tfrac{1}{2}(n-3)\tilde{S}'\tilde{S}'+\tilde{S}\tilde{S}''](4x^2F''-4xF')=0 \qquad (2.11)$$

where

$$\tilde{S}=\tfrac{1}{4}(S_r-S_\theta)^2+S_{r\theta}^2.$$

Method of solution

(*a*) *Plane stress.* Rewrite equation (2.6) as

$$2c_1(x^4F''''+2x^3F'''-x^2F''+xF'-2xF'''+4F''+F'''''+2x^2F'''')$$
$$+c_2(2x^2F-3x^3F'+2x^4F''-x^2F'')$$
$$+c_3(4x^4F'''+x^3F''+4x^2F'''+2xF-4xF''-2x^2F')$$
$$+2c_4(2x^2F'''-3xF''+5F'+2F''')$$
$$+c_5(2F+2F''-x^2F'')+6c_6(x^2F''-xF')=0 \qquad (2.12)$$

where

$$c_1 = 1 + p\bar{S}^{\frac{1}{2}(n-1)}$$
$$c_2 = \tfrac{1}{2}(n-1)p\bar{S}^{\frac{1}{2}(n-5)}[\tfrac{1}{2}(n-3)\bar{S}'^2 + \bar{S}\bar{S}'']$$
$$c_3 = \tfrac{1}{2}(n-1)p\bar{S}^{\frac{1}{2}(n-5)}\bar{S}\bar{S}'$$
$$c_4 = \tfrac{1}{2}(n-1)p\bar{S}^{\frac{1}{2}(n-5)}\bar{S}\bar{S}^{\cdot}$$
$$c_5 = \tfrac{1}{2}(n-1)p\bar{S}^{\frac{1}{2}(n-5)}[\tfrac{1}{2}(n-3)\bar{S}^{\cdot 2} + \bar{S}\bar{S}^{\cdot\cdot}]$$
$$c_6 = \tfrac{1}{2}(n-1)p\bar{S}^{\frac{1}{2}(n-5)}[\tfrac{1}{2}(n-3)\bar{S}^{\cdot}\bar{S}' + \bar{S}\bar{S}'^{\cdot}].$$

Equation (2.8) (for $p = \infty$) can also be written in the form (2.12), with

$$c_1 = \bar{S}^2$$
$$c_2 = \tfrac{1}{2}(n-1)[\tfrac{1}{2}(n-3)\bar{S}'^2 + \bar{S}\bar{S}'']$$
$$c_3 = \tfrac{1}{2}(n-1)\bar{S}\bar{S}'$$
$$c_4 = \tfrac{1}{2}(n-1)\bar{S}\bar{S}^{\cdot}$$
$$c_5 = \tfrac{1}{2}(n-1)[\tfrac{1}{2}(n-3)\bar{S}^{\cdot 2} + \bar{S}\bar{S}^{\cdot\cdot}]$$
$$c_6 = \tfrac{1}{2}(n-1)[\tfrac{1}{2}(n-3)\bar{S}^{\cdot}\bar{S}' + \bar{S}\bar{S}'^{\cdot}].$$

Let the direction $\theta = 0$ coincide with one of the principal axes of the applied load; then the solution can be expanded into a fourier series of the form

$$F = \sum_{m=0,2,4,\ldots}^{\infty} f_m(x)\cos m\theta.$$

Substitution into equation (2.12) gives

$$\sum_{m=0,2,4,\ldots}^{\infty} (A_{4m}f_m'''' + A_{3m}f_m''' + A_{2m}f_m'' + A_{1m}f_m' + A_{0m}f_m) = 0 \qquad (2.13)$$

where

$$A_{4m} = 2c_1x^4\cos m\theta$$
$$A_{3m} = 4x^3(c_1 + xc_3)\cos m\theta$$
$$A_{2m} = x^2[\{-2c_1(1+2m^2) + 2c_2x^2 + c_3x - c_5\}\cos m\theta - 4mc_4\sin m\theta]$$
$$A_{1m} = x[\{2(c_1 - c_3x)(1+2m^2) - 3c_2x^2\}\cos m\theta - 6m(c_6x - c_4)\sin m\theta]$$
$$A_{0m} = \{2c_1m^2(m^2-4) + c_2x^2(2+m^2) + 2c_3x(1+2m^2) + 2c_5(1-m^2)\}\cos m\theta$$
$$+ \{6c_6xm - 2c_4m(5-2m^2)\}\sin m\theta.$$

Here the A's are even functions of θ, and can be represented by cosine series as

$$A_{st} = \sum_{j=0,2,4,\ldots}^{\infty} B_{st}^j(x)\cos j\theta.$$

Substitute into equation (2.13) and let the coefficient of $\cos j\theta$ equal zero. A set of ordinary differential equations is obtained as

$$\sum_{m=0,2,4,\ldots}^{\infty} (B_{4m}^j f_m'''' + B_{3m}^j f_m''' + B_{2m}^j f_m'' + B_{1m}^j f_m' + B_{0m}^j f_m) = 0 \qquad \text{for } j = 0, 2, 4, \ldots \qquad (2.14)$$

where the B_{st}^j are determined by

$$B_{st}^j = \frac{4}{(1+\delta_{0j})\pi}\int_0^{\pi/2} A_{st}\cos j\theta \, d\theta. \tag{2.15}$$

If a finite number of terms in the fourier series is taken, equation (2.14) might conceivably be solved by an iterative process. First calculate B_{st}^j by using an approximate solution (usually the elastic solution is taken for the first try) and solve the equations by Potters' method [13], which is described in Appendix A. Then with the new approximate solution recalculate the B_{st}^j by formula (2.15) and solve the equations again. Continue the process until, hopefully, the solution converges.

For n large or when many terms are taken in the fourier series, this iterative procedure is usually found not to converge. A more efficient iteration technique, to be described next, has to be employed.

Recall Newton's method. Let $G(F) = 0$ be the governing equation, and suppose that F is an approximate solution. Then a better solution is

$$F^* = F + \delta F$$

where δF is obtained from the equation

$$\delta G(F) = -G(F). \tag{2.16}$$

Continue the process until δF becomes sufficiently small.

Now write equation (2.12) as

$$G(F) = c_1L_1 + c_2L_2 + c_3L_3 + c_4L_4 + c_5L_5 + c_6L_6 = 0$$

where

$$\begin{aligned}
L_1 &= 2(x^4F'''' + 2x^3F''' - x^2F'' + xF' - 2xF''' + 4F'' + F'''' + 2x^2F'''')\\
L_2 &= 2x^2F - 3x^3F' + 2x^4F'' - x^2F''\\
L_3 &= 4x^4F''' + x^3F'' - 2x^2F' + 4x^2F''' + 2xF - 4xF''\\
L_4 &= 2(2x^2F''' - 3xF'' + 5F' + 2F'''')\\
L_5 &= 2F + 2F'' - x^2F''\\
L_6 &= 6(x^2F'' - xF').
\end{aligned}$$

Then the equation corresponding to equation (2.16) is

$$\begin{aligned}
&c_1\delta L_1 + c_2\delta L_2 + c_3\delta L_3 + c_4\delta L_4 + c_5\delta L_5 + c_6\delta L_6\\
&\quad + L_1\delta c_1 + L_2\delta c_2 + L_3\delta c_3 + L_4\delta c_4 + L_5\delta c_5 + L_6\delta c_6 = -G.
\end{aligned}$$

Carry out all the variations, and this equation can be written as

$$\begin{aligned}
&d_1\delta F'''' + d_2\delta F''' + d_3\delta F'''' + d_4\delta F'' + d_5\delta F''' + d_6\delta F'''' + d_7\delta F' + d_8\delta F'' + d_9\delta F'''\\
&\quad + d_{10}\delta F'''' + d_{11}\delta F + d_{12}\delta F' + d_{13}\delta F'' + d_{14}\delta F''' + d_{15}\delta F'''' = -G
\end{aligned} \tag{2.17}$$

where the d's are given in Appendix B. Let

$$\delta F = \sum_{m=0,2,4,\ldots} \delta f_m(x)\cos m\theta.$$

Equation (2.17) becomes

$$\sum_{m=0,2,4,\ldots} (a_{4m}\,\delta f''''_m + a_{3m}\,\delta f'''_m + a_{2m}\,\delta f''_m + a_{1m}\,\delta f'_m + a_{0m}\,\delta f_m) = -G \tag{2.18}$$

where

$$\begin{aligned}
a_{4m} &= d_1 \cos m\theta \\
a_{3m} &= d_2 \cos m\theta - m d_3 \sin m\theta \\
a_{2m} &= d_4 \cos m\theta - m d_5 \sin m\theta - m^2 d_6 \cos m\theta \\
a_{1m} &= d_7 \cos m\theta - m d_8 \sin m\theta - m^2 d_9 \cos m\theta + m^3 d_{10} \sin m\theta \\
a_{0m} &= d_{11} \cos m\theta - m d_{12} \sin m\theta - m^2 d_{13} \cos m\theta + m^3 d_{14} \sin m\theta + m^4 d_{15} \cos m\theta.
\end{aligned}$$

The quantities a_{st}, G are even functions of θ, and can be represented by cosine series as

$$\begin{aligned}
a_{st} &= \sum_{j=0,2,4,\ldots} b_{st}^j \cos j\theta \\
G &= \sum_{j=0,2,4,\ldots} G^j \cos j\theta.
\end{aligned}$$

Substitute into (2.18), and let the coefficient of $\cos j\theta$ equal zero. A set of ordinary differential equations is obtained as

$$\sum_{m=0,2,4,\ldots} (b_{4m}^j\,\delta f''''_m + b_{3m}^j\,\delta f'''_m + b_{2m}^j\,\delta f''_m + b_{1m}^j\,\delta f'_m + b_{0m}^j\,\delta f_m) = -G^j \qquad \text{for } j = 0, 2, 4, \ldots J \tag{2.19}$$

where the b_{st}^j, G^j are determined by

$$\begin{aligned}
b_{st}^j &= \frac{4}{(1+\delta_{0j})\pi} \int_0^{\pi/2} a_{st} \cos j\theta \, \mathrm{d}\theta \\
G^j &= \frac{4}{(1+\delta_{0j})\pi} \int_0^{\pi/2} G \cos j\theta \, \mathrm{d}\theta.
\end{aligned} \tag{2.20}$$

Calculate b_{st}^j, G^j by using an approximate solution

$$F = \sum_{m=0,2,4,\ldots} f_m(x) \cos m\theta$$

and solve for δf_m by Potters' method. Then a better solution is

$$F^* = \sum_{m=0,2,4,\ldots} f_m^*(x) \cos m\theta$$

where

$$f_m^* = f_m + \delta f_m.$$

Recalculate b_{st}^j, G^j, and solve the equations again. Continue the procedure until δf_m becomes sufficiently small.

It may be noted that for the calculation of the B_{st}^j, b_{st}^j, G^j, it is very difficult to obtain analytic values, unless only one or two terms are taken in the fourier series. Instead, numerical values were calculated from the integral formulas (2.15), (2.20) at each mesh point used in the Potters' method.

If the loading is pure shear applied at infinity, it is convenient to expand F in the sine series

$$F = \sum_{m=2,6,10,\ldots} f_m(x) \sin m\theta. \tag{2.21}$$

Then the expressions of the A_{st} in equation (2.13) are

$$A_{4m} = 2c_1 x^4 \sin m\theta$$

$$A_{3m} = 4x^3(c_1 + c_3 x) \sin m\theta$$

$$A_{2m} = x^2[\{-2c_1(1+2m^2) + 2c_2 x^2 + c_3 x - c_5\} \sin m\theta + 4mc_4 \cos m\theta]$$

$$A_{1m} = x[\{2(c_1 - c_3 x)(1+2m^2) - 3c_2 x^2\} \sin m\theta + 6m(c_6 x - c_4) \cos m\theta]$$

$$A_{0m} = [2c_1 m^2(m^2-4) + c_2 x^2(2+m^2) + 2c_3 x(1+2m^2) + 2c_5(1-m^2)] \sin m\theta$$
$$+ [2c_4 m(5-2m^2) - 6c_6 xm] \cos m\theta$$

which, again, can be represented by

$$A_{st} = \sum_{j=2,6,10,\ldots} B_{st}^j(x) \sin j\theta.$$

Similarly, the expansions of δF, a_{st}, G in Newton's method are

$$\delta F = \sum_{m=2,6,10,\ldots} \delta f_m(x) \sin m\theta$$

$$a_{st} = \sum_{j=2,6,10,\ldots} b_{st}^j \sin j\theta$$

and

$$G = \sum_{j=2,6,10,\ldots} G^j \sin j\theta$$

where the a_{st} are given by

$$a_{4m} = d_1 \sin m\theta$$

$$a_{3m} = d_2 \sin m\theta + md_3 \cos m\theta$$

$$a_{2m} = d_4 \sin m\theta + md_5 \cos m\theta - m^2 d_6 \sin m\theta$$

$$a_{1m} = d_7 \sin m\theta + md_8 \cos m\theta - m^2 d_9 \sin m\theta - m^3 d_{10} \cos m\theta$$

$$a_{0m} = d_{11} \sin m\theta + md_{12} \cos m\theta - m^2 d_{13} \sin m\theta - m^3 d_{14} \cos m\theta + m^4 d_{15} \sin m\theta$$

and the d's are the same as before.

(b) *Plane strain.* Equations (2.9) and (2.11) can also be solved by the method just described above. In equation (2.9), the approximate value of $\hat{S}$ in each iteration may be obtained from expression (2.10) with the use of the previous $\hat{S}$ for the value on the right hand side. In the present study, only equation (2.11) is considered for the case of pure shear loading. In this case, the expressions for the A_{st} and d's are given in Appendix B.

3. STRESS CONCENTRATION AT A CIRCULAR HOLE IN AN INFINITE PLATE SUBJECTED TO LOADS IN ITS OWN PLANE

Plate with a hole in pure tension

(a) *Governing equations and boundary conditions.* The loading related to the polar coordinates is shown in Fig. 1. Assume that the strain is small and the thickness of the plate remains constant during deformation. The stress components transverse to the plate are assumed negligible, and so the stress field in the plate is approximated by a state of plane stress. Then equation (2.6) is the governing equation for λ finite and equation (2.8) is for λ infinite.

From the symmetry conditions, the modified stress function is in the form

$$F = \sum_{m=0,2,4,\ldots} f_m(x) \cos m\theta.$$

The boundary conditions at the hole are

$$S_r = 0, \qquad S_{r\theta} = 0$$

or

$$\begin{aligned} 2F(1) - F'(1) + F'''(1) &= 0 \\ F''(1) - F'(1) &= 0 \end{aligned} \tag{3.1}$$

and the stresses at infinity are

$$\begin{aligned} S_r &= \tfrac{1}{2}(1 + \cos 2\theta) \\ S_\theta &= \tfrac{1}{2}(1 - \cos 2\theta) \\ S_{r\theta} &= -\tfrac{1}{2} \sin 2\theta. \end{aligned}$$

These give

$$F(0) = \tfrac{1}{4} - \tfrac{1}{4} \cos 2\theta. \tag{3.2}$$

In order to obtain the second boundary condition at $x = 0$, rewrite equation (2.3) as

$$x\varepsilon_\theta'' + \varepsilon_r' + 2\varepsilon_{r\theta}'' = \frac{-\varepsilon_r''' + 2\dot{\varepsilon}_{r\theta}}{x}.$$

At $x = 0$, $-\varepsilon_r''' + 2\dot{\varepsilon}_{r\theta} = 0$; so this gives

$$\varepsilon_r'''(0) + \varepsilon_r'(0) = 0.$$

But since ε_r has the form $\varepsilon_r = \sum_{m=0,2,4,\ldots} h_m(x) \cos m\theta$, it follows that

$$\varepsilon_r'(0) = 0.$$

Hence, from the stress–strain relation (2.5), we have

$$F'(0) + F'''(0) = 0.$$

Again, F has the form $F = \sum_{m=0,2,4,\ldots} f_m(x) \cos m\theta$; so the second boundary condition at infinity is

$$F'(0) = 0. \tag{3.3}$$

It is noted that the boundary conditions (3.1) only give one condition for $f_0(1)$, and the second condition is obtained by letting $f_0(1)$ equal an arbitrary constant.

(b) *Results and discussion.* Equation (2.6) [or (2.8) for $\lambda = \infty$] with boundary conditions (3.1), (3.2) and (3.3) was solved by Newton's method described in Section 2. Calculations were made for values of $n = 3, 5$ and 9. Depending on λ and n, from three to six terms in

the fourier series (with the same number of terms for the expansions of δF and a_{st}) were found to be needed for satisfactory convergence. Convergence was considered to be satisfactory, if the difference of the results for the stress concentration factor was less than 1 per cent when an additional term was added.

The results for stress concentration factors determined as $K = [(\sigma_\theta)_{a,\pi/2}]/\sigma_\infty$ are shown in Fig. 6 as plots of K against λ for $\lambda < 1$ and against $1/\lambda$ for $\lambda > 1$. The limiting result for

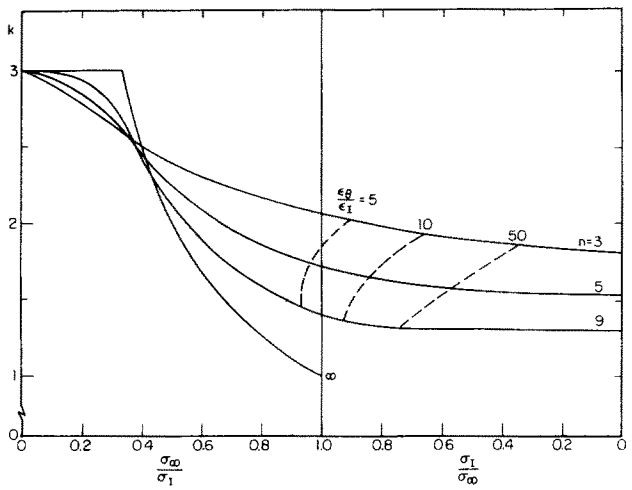

FIG. 6. Variation of stress concentration factor with applied stress.

$n = \infty$, corresponding to an elastic–ideally plastic material was obtained by assuming that the maximum stress at the hole is $3\sigma_\infty$ until σ_∞ reaches $\frac{1}{3}\sigma_I$ and thereafter remains at the value σ_I. Thus, for $\frac{1}{3}\sigma_I < \sigma_\infty < \sigma_I$ the stress concentration factor is $K = 1/\lambda$. It may be noted that σ_∞ can not exceed σ_I for an ideally plastic material. The dashed lines shown in this figure connect points of constant $[(\varepsilon_\theta)_{a,\pi/2}]/\varepsilon_I$, where ε_I is the nominal yield strain associated with σ_I; that is $\varepsilon_I = 10/7\,\sigma_I/E$. Since the stress state at the hole is uniaxial, $[(\varepsilon_\theta)_{a,\pi/2}]/\varepsilon_I$ is obtained simply from the Ramberg–Osgood relation (2.1) as

$$\frac{(\varepsilon_\theta)_{a,\pi/2}}{\varepsilon_I} = 0{\cdot}7\lambda K + 0{\cdot}3(\lambda K)^n. \tag{3.4}$$

Figure 7 shows the stress history at the point of the maximum stress (i.e. at $\theta = \pi/2$, $r = a$).

Figures 8(a)–10(b) show the distributions of σ_θ and $\hat{\sigma}$ along $\theta = \pi/2$ for $\lambda = 0{\cdot}3$, $0{\cdot}8$ and ∞. It is interesting to note that the maximum stress σ_θ no longer occurs at the hole when the deformation becomes large; but the effective stress still attains its maximum at the hole.

A typical distribution of $\hat{\sigma}$ in the plastic range is shown in Fig. 11(a) wherein contours of constant values of $\hat{\sigma}$ are plotted for the case $n = 9$ and $\lambda = 0{\cdot}8$. For comparison, similar contours are shown for the elastic case in Fig. 11(b). A detailed stress distribution for $\lambda = 0{\cdot}8$ and $n = 9$ is given in Table 1.

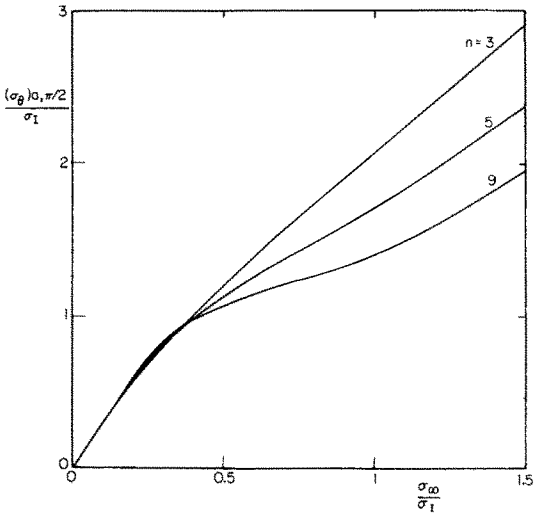

FIG. 7. Stress history at the point of maximum stress.

In order to check the acceptability of the J_2 deformation theory, the stress paths at various points along $\theta = \pi/2$ (which appear to deviate the most from proportional loading) for $n = 3$ and $n = 9$ are shown in Figs. 12 and 13, respectively. These plots show that the stress paths depart only slightly from a radial direction by amounts which are well within the permissible range given by the criterion of Ref. [12].

It may be interesting to compare the present results with Budiansky and Videnšek's. They also used the Ramberg–Osgood relation and expanded the stress function into fourier series, but only two terms were taken. The comparison of the stress concentration factor is shown in Table 2. It can be seen that their results agree with our two terms' results fairly well.

Plate with a hole in pure shear

(a) *Governing equations and boundary conditions.* The loading related to the coordinate system is shown in Fig. 2. As in the case of pure tension, the usual assumptions of generalized plane stress are made, with strain assumed small and changes in the plate thickness neglected. Equations (2.6) and (2.8) are then the governing equation for λ finite and infinite, respectively.

The modified stress function F is assumed in the form (2.21). The stress components at infinity are

$$S_r = \sin 2\theta$$

$$S_\theta = -\sin 2\theta$$

$$S_{r\theta} = \cos 2\theta.$$

These give

$$F(0) = -\tfrac{1}{2}\sin 2\theta. \tag{3.5}$$

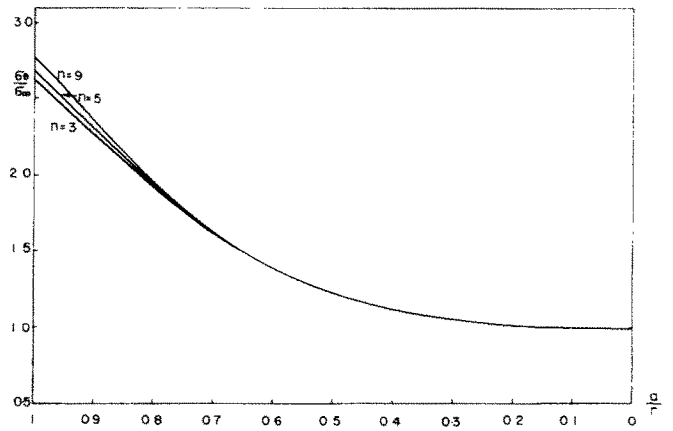

FIG. 8(a). Stress distribution of σ_θ along $\theta = \pi/2$ for $\lambda = 0{\cdot}3$.

As in the case of pure tension, it can easily be shown that the second boundary condition at infinity is

$$F'(0) = 0. \tag{3.6}$$

The boundary conditions at the hole remain as same as (3.1).

(b) *Results and discussion.* As in the previous case, equation (2.6) [or (2.8) for $\lambda = \infty$] with boundary conditions (3.5), (3.6) and (3.1) was solved for values of $n = 3$, 5 and 9. Two to five terms in the fourier series were found to be needed for satisfactory convergence (on the basis of the same convergence criterion as in the tension case). The results for the stress concentration factor defined as $K = [(\sigma_\theta)_{a,\pi/4}]/\tau_\infty$ are shown in Fig. 14. The limiting result for $n = \infty$ was obtained by assuming that the maximum stress at the hole is $4\tau_\infty$ until τ_∞ reaches $\frac{1}{4}\sigma_I$, and thereafter remains at the value σ_I. Thus, for $\frac{1}{4}\sigma_I < \tau_\infty < 1/\sqrt{(3)}\sigma_I$ the stress concentration factor is $K = 1/\lambda$. It may be noted that τ_∞ cannot exceed $1/\sqrt{(3)}\sigma_I$ for an ideally plastic material obeying the Mises yield criterion. Again the dashed lines in

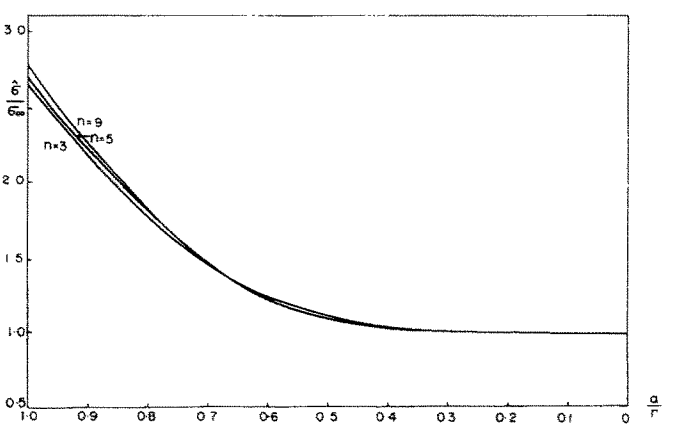

FIG. 8(b). Stress distribution of $\hat{\sigma}$ along $\theta = \pi/2$ for $\lambda = 0{\cdot}3$.

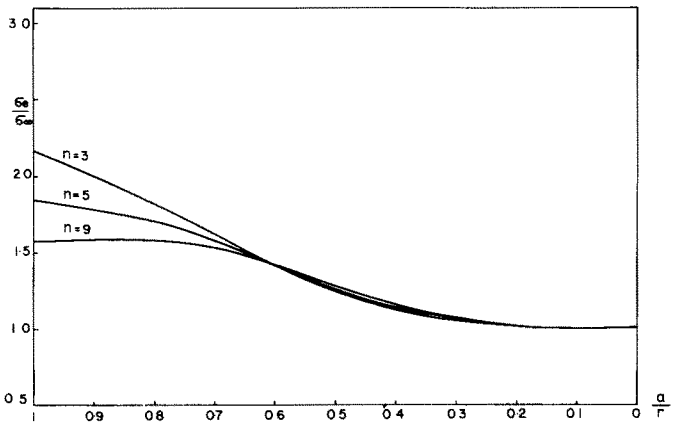

FIG. 9(a). Stress distribution of σ_θ along $\theta = \pi/2$ for $\lambda = 0{\cdot}8$.

this figure connect points of constant strain $[(\varepsilon_\theta)_{a,\pi/4}]/\varepsilon_I$, as obtained from the Ramberg–Osgood relation (2.1).

The stress history at the point of maximum stress (i.e. at $\theta = \pi/4$, $r = a$) is shown in Fig. 15.

Figures 16(a)–18(b) show the stress distributions of σ_θ and $\hat{\sigma}$ along $\theta = \pi/4$ for $\lambda = 0{\cdot}2$, $0{\cdot}7$ and ∞. As in the pure tension case, the maximum stress does not necessarily occur at the hole, but the effective stress does reach its maximum at the hole. It is interesting to note that the effective stress $\hat{\sigma}$ attains a minimum at about $r = 2a$, which does not occur in the case of pure tension.

A typical distribution of $\hat{\sigma}$ in the plastic range is shown in Fig. 19(a), wherein contours of constant values of $\hat{\sigma}$ are plotted for the case of $n = 9$ and $\lambda = 0{\cdot}7$. For comparison, similar contours are shown for the elastic case in Fig. 19(b). A detailed stress distribution for $\lambda = 0{\cdot}7$ and $n = 9$ is given in Table 3.

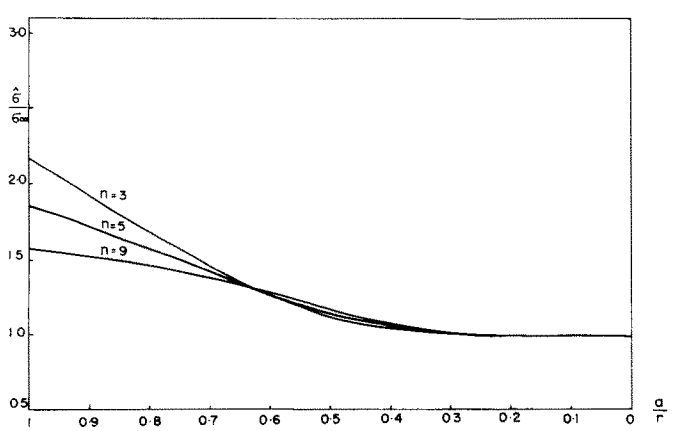

FIG. 9(b). Stress distribution of $\hat{\sigma}$ along $\theta = \pi/2$ for $\lambda = 0{\cdot}8$.

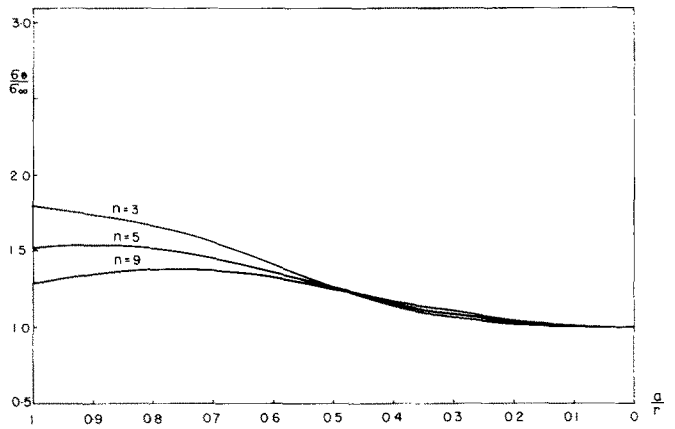

FIG. 10(a). Stress distribution of σ_θ along $\theta = \pi/2$ for $\lambda = \infty$.

The stress paths at various points along $\theta = \pi/4$ (which appear to deviate the most from proportional loading) for $n = 3$ and $n = 9$ are shown in Figs. 20 and 21, respectively. Figure 21 shows that the stress path at $a/r = 0{\cdot}6$ has a serious deviation from proportional loading in the range of $\hat{\sigma} < \sigma_I$ bounded by the dashed line. But plastic strains are so small in this range that we may expect the present deformation-theory analysis still give a reasonable solution to the problem.

4. ON STOWELL'S FORMULA AND NEUBER'S RULE

Stowell's formula

Stowell [9] presented an approximate formula for the stress concentration factor at a circular hole in an infinite plate under pure tension as

$$K = 1 + 2\frac{(E_s)_{a,\pi/2}}{(E_s)_\infty} \tag{4.1}$$

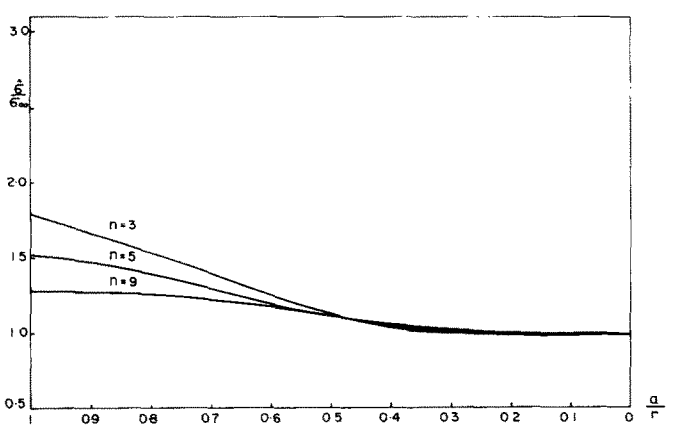

FIG. 10(b). Stress distribution of $\hat{\sigma}$ along $\theta = \pi/2$ for $\lambda = \infty$.

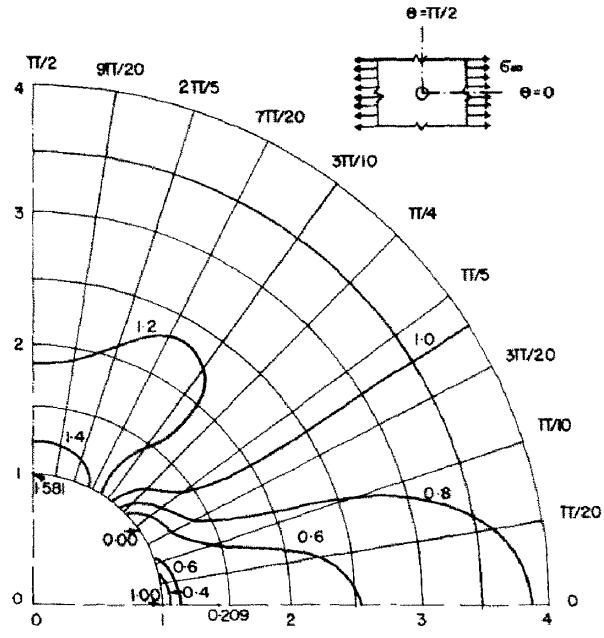

FIG. 11(a). Effective stress distribution for $\lambda = 0{\cdot}8$ and $n = 9$.

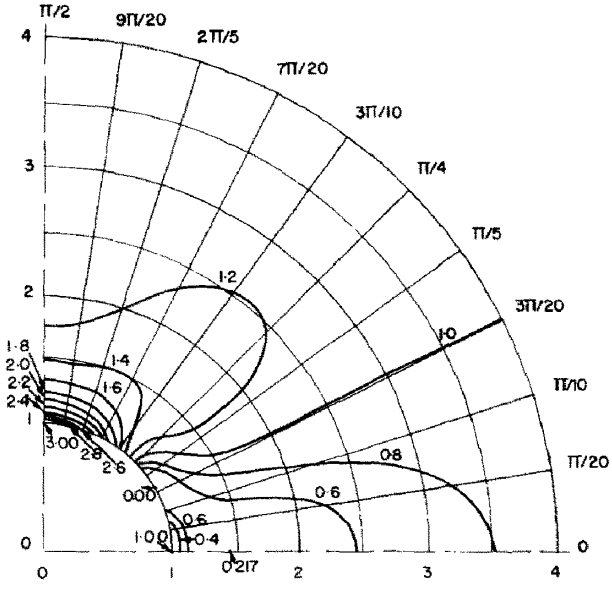

FIG. 11(b). Effective stress distributions in the elastic range.

TABLE 1. STRESS DISTRIBUTIONS IN A PURE TENSION PLATE FOR $n = 9$ AND $\lambda = 0{\cdot}8$

a/r \ θ	0	$\pi/20$	$\pi/10$	$3\pi/20$	$\pi/5$	$\pi/4$	$3\pi/10$	$7\pi/20$	$2\pi/5$	$9\pi/20$	$\pi/2$
(a) S_r											
0·0	1·000	0·976	0·905	0·794	0·655	0·500	0·346	0·206	0·096	0·025	0·000
0·1	0·970	0·945	0·873	0·762	0·626	0·482	0·343	0·218	0·117	0·049	0·025
0·2	0·884	0·861	0·792	0·686	0·561	0·440	0·335	0·245	0·167	0·108	0·086
0·3	0·756	0·736	0·678	0·586	0·477	0·380	0·311	0·263	0·223	0·188	0·173
0·4	0·597	0·584	0·544	0·474	0·389	0·317	0·273	0·259	0·264	0·276	0·281
0·5	0·420	0·417	0·399	0·358	0·304	0·256	0·228	0·234	0·283	0·351	0·384
0·6	0·246	0·249	0·251	0·246	0·227	0·199	0·182	0·207	0·288	0·385	0·430
0·7	0·099	0·100	0·114	0·142	0·158	0·146	0·141	0·187	0·277	0·359	0·390
0·8	−0·007	−0·006	0·012	0·055	0·091	0·099	0·111	0·162	0·231	0·274	0·286
0·9	−0·050	−0·046	−0·030	0·001	0·032	0·054	0·076	0·107	0·136	0·149	0·151
1·0	0·000	0·000	0·000	0·000	0·000	0·000	0·000	0·000	0·000	0·000	0·000
(b) S_θ											
0·0	0·000	0·025	0·096	0·206	0·346	0·500	0·655	0·794	0·905	0·976	1·000
0·1	0·006	0·030	0·101	0·212	0·352	0·507	0·662	0·802	0·913	0·984	1·009
0·2	0·018	0·043	0·115	0·227	0·370	0·528	0·687	0·830	0·943	1·015	1·040
0·3	0·031	0·056	0·130	0·246	0·393	0·558	0·725	0·876	0·994	1·068	1·093
0·4	0·036	0·063	0·140	0·262	0·417	0·591	0·768	0·930	1·061	1·144	1·173
0·5	0·021	0·051	0·138	0·269	0·436	0·623	0·812	0·989	1·142	1·252	1·293
0·6	−0·033	0·004	0·106	0·258	0·446	0·651	0·859	1·059	1·242	1·381	1·434
0·7	−0·145	−0·103	0·019	0·210	0·438	0·674	0·912	1·148	1·353	1·491	1·539
0·8	−0·339	−0·290	−0·141	0·099	0·388	0·687	0·979	1·245	1·449	1·557	1·587
0·9	−0·641	−0·573	−0·380	−0·088	0·278	0·679	1·051	1·333	1·501	1·577	1·597
1·0	−1·007	−0·932	−0·712	−0·351	0·137	0·671	1·113	1·379	1·503	1·561	1·581
(c) $S_{r\theta}$											
0·0	0·000	−0·155	−0·294	−0·405	−0·476	−0·500	−0·476	−0·405	−0·294	−0·155	0·000
0·1	0·000	−0·158	−0·301	−0·415	−0·489	−0·515	−0·491	−0·417	−0·303	−0·159	0·000
0·2	0·000	−0·168	−0·318	−0·438	−0·516	−0·545	−0·521	−0·445	−0·324	−0·171	0·000
0·3	0·000	−0·179	−0·340	−0·465	−0·545	−0·573	−0·549	−0·474	−0·351	−0·187	0·000
0·4	0·000	−0·191	−0·361	−0·490	−0·569	−0·592	−0·564	−0·491	−0·372	−0·204	0·000
0·5	0·000	−0·199	−0·375	−0·507	−0·581	−0·596	−0·562	−0·486	−0·367	−0·201	0·000
0·6	0·000	−0·196	−0·375	−0·507	−0·574	−0·580	−0·538	−0·450	−0·318	−0·161	0·000
0·7	0·000	−0·179	−0·345	−0·471	−0·535	−0·536	−0·481	−0·372	−0·232	−0·102	0·000
0·8	0·000	−0·147	−0·277	−0·380	−0·443	−0·445	−0·374	−0·256	−0·139	−0·055	0·000
0·9	0·000	−0·091	−0·165	−0·226	−0·273	−0·274	−0·212	−0·124	−0·059	−0·024	0·000
1·0	0·000	0·000	0·000	0·000	0·000	0·000	0·000	0·000	0·000	0·000	0·000
(d) $\hat{S}$											
0·0	1·000	1·000	1·000	1·000	1·000	1·000	1·000	1·000	1·000	1·000	1·000
0·1	0·967	0·970	0·977	0·990	1·006	1·020	1·025	1·019	1·008	0·999	0·996
0·2	0·875	0·889	0·924	0·971	1·021	1·063	1·081	1·068	1·037	1·010	1·000
0·3	0·741	0·775	0·857	0·954	1·042	1·109	1·141	1·131	1·089	1·040	1·018
0·4	0·579	0·647	0·793	0·943	1·065	1·146	1·187	1·190	1·153	1·093	1·061
0·5	0·410	0·524	0·739	0·936	1·078	1·166	1·214	1·229	1·211	1·171	1·150
0·6	0·264	0·420	0·685	0·914	1·066	1·158	1·218	1·246	1·253	1·265	1·275
0·7	0·212	0·356	0·607	0·837	1·003	1·112	1·190	1·247	1·302	1·359	1·385
0·8	0·335	0·384	0·502	0·664	0·844	1·003	1·132	1·255	1·369	1·442	1·465
0·9	0·618	0·573	0·464	0·402	0·542	0·807	1·079	1·300	1·441	1·509	1·527
1·0	1·007	0·932	0·712	0·351	0·137	0·671	1·113	1·379	1·503	1·561	1·581

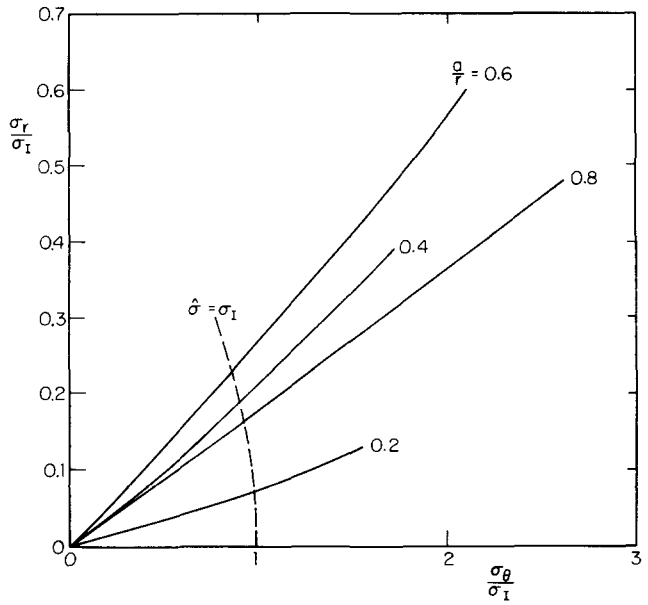

FIG. 12. Stress history at fixed points along $\theta = \pi/2$ for $n = 3$.

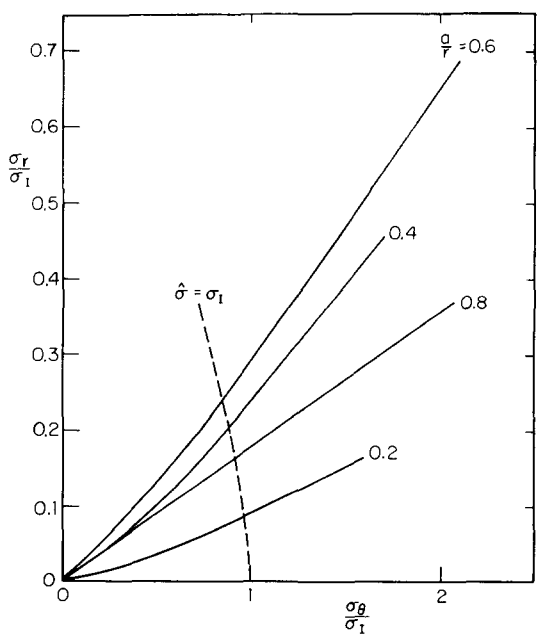

FIG. 13. Stress history at fixed points along $\theta = \pi/2$ for $n = 9$.

TABLE 2. A COMPARISON OF THE STRESS CONCENTRATION FACTOR BETWEEN PRESENT RESULTS AND BUDIANSKY AND VIDENSEK

		K		
		Present		Budiansky and Videnšek
	λ	Final result ($M = 4$)†	Two terms ($M = 2$)	($M = 2$)
	0·3	2·65	2.73	2·80
$n = 3$	0·5	2·40	2·52	2·60
	0·8	2·17	2·32	2·43
		($M = 5$)		
	0·3	2·68	2·76	2·80
$n = 5$	0·5	2·24	2·35	2·40
	0·8	1·85	1·97	2·00
		($M = 6$)		
	0·3	2·79	2·86	2·95
$n = 9$	0·5	2·13	2·24	2·25
	0·8	1·58	1·67	1·68

† M is the number of terms taken for the fourier series expansions.

where K is the stress concentration factor defined as $K = [(\sigma_\theta)_{a,\pi/2}]/\sigma_\infty$, $(E_s)_{a,\pi/2}$ is the secant modulus at the point of maximum stress and $(E_s)_\infty$ is the secant modulus at points far away from the hole where the stress is applied.

This formula was obtained from an approximate stress distribution which was adjusted by minimizing the mean square of the error in satisfying the equilibrium equations. There was no consideration of the compatibility equations. This analysis is questionable in several respects, but Stowell's formula is often used because of its simplicity and good agreement with many experimental results.

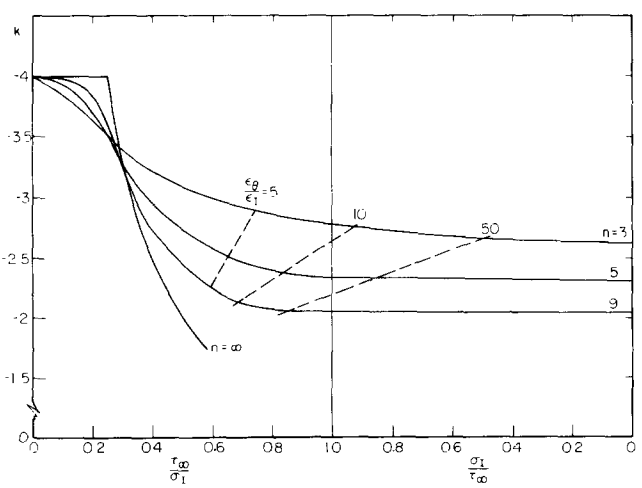

FIG. 14. Variation of stress concentration factor with applied stress.

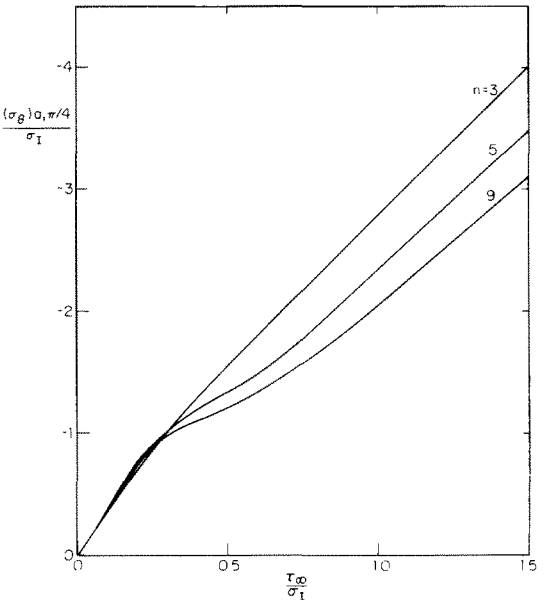

FIG. 15. Stress history at the point of maximum stress.

A comparison of the stress concentration factors obtained from this formula and the results presented in the last section is given in Table 4, in which the Ramberg–Osgood stress–strain curve was used and formula (4.1) becomes

$$K = 1+\frac{2(1+\frac{3}{7}\lambda^{n-1})}{1+\frac{3}{7}\lambda^{n-1}K^{n-1}}. \tag{4.2}$$

It is rather surprising that Stowell's formula gives results that agree so closely with those obtained by the present analysis.

Formula for the stress concentration factor in a pure shear plate with a circular hole

Following Stowell's derivation for a tension plate, a formula for the stress concentration factor at a circular hole in an infinite plate under pure shear is obtained in Appendix C as

$$\hat{K} = 1+\left(\frac{4}{\sqrt{3}}-1\right)\frac{(E_s)_{a,\pi/4}}{(E_s)_\infty} \tag{4.3}$$

where $\hat{K}$ is the stress concentration factor defined as $\hat{K} = [(\hat{\sigma}_\theta)_{a,\pi/4}]/\hat{\sigma}_\infty$, $(E_s)_{a,\pi/4}$ is the secant modulus at the point of maximum stress and $(E_s)_\infty$ is the secant modulus at infinity.

As mentioned in the previous section, it can be seen that this formula is achieved on the basis of a treatment that ignores compatibility entirely and satisfies equilibrium in some average fashion. It is desirable to assess this formula by comparing the results with those obtained from the previous numerical analysis. Let us reintroduce the stress concentration factor $K = [(\sigma_\theta)_{a,\pi/4}]/\tau_\infty$, and use the Ramberg–Osgood uniaxial curve to determine the secant modulus. Then formula (4.3) becomes

$$K = -\sqrt{3}-(4-\sqrt{3})\frac{1+\frac{3}{7}\sqrt{(3)}^{n-1}\lambda^{n-1}}{1+\frac{3}{7}\lambda^{n-1}K^{n-1}}. \tag{4.4}$$

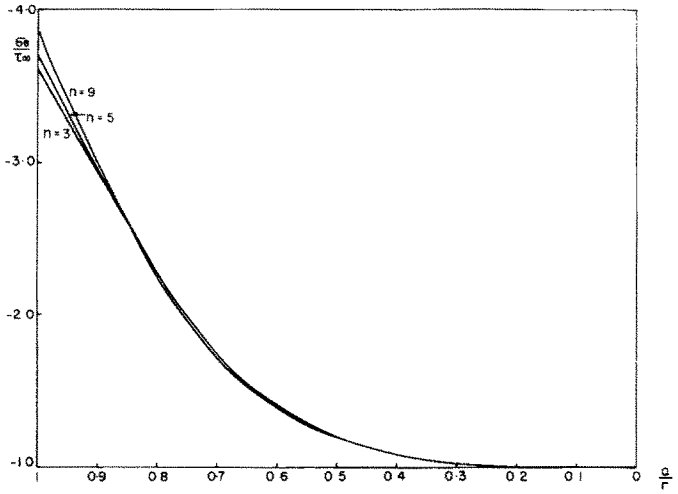

FIG. 16(a). Stress distribution of σ_θ along $\theta = \pi/4$ for $\lambda = 0{\cdot}2$.

The results are given in Table 5. It is seen that this formula gives slightly higher results than those obtained from the numerical analysis, but the difference is small. The formula is therefore reasonably good for an approximate estimate of the stress concentration factor in a pure shear plate with a circular hole.

Generalized formula for a plate with arbitrary holes, notches or fillets

Based on experimental results, Hardrath and Ohman [10] generalized Stowell's formula for arbitrary holes, notches or fillets in a tension plate by rewriting formula (4.1) as

$$K_{\text{plastic}} = 1 + (K_{\text{elastic}} - 1)\frac{(E_s)_{\text{max stress}}}{(E^s)_\infty} \tag{4.5}$$

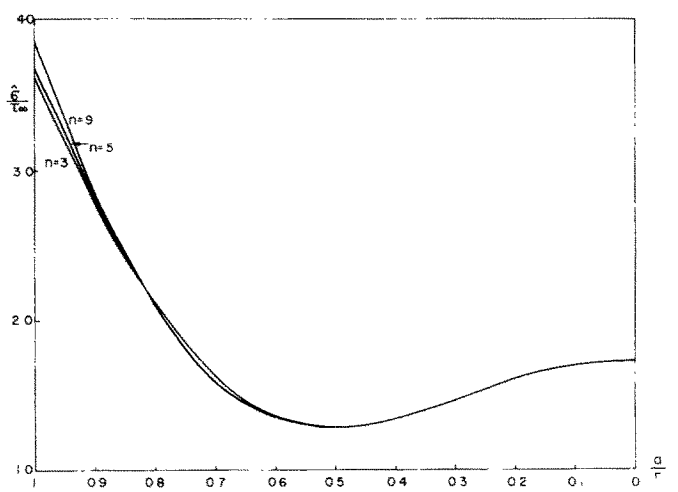

FIG. 16(b). Stress distribution of $\hat{\sigma}$ along $\theta = \pi/4$ for $\lambda = 0{\cdot}2$.

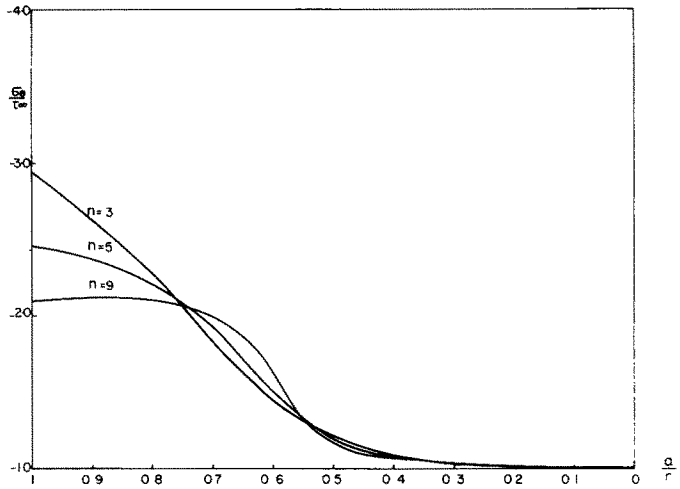

FIG. 17(a). Stress distribution of σ_θ along $\theta = \pi/4$ for $\lambda = 0{\cdot}7$.

where K_{plastic} is the stress concentration factor in the plastic range and K_{elastic} is the stress concentration factor in the elastic range.

Similarly, by inserting a corresponding value of $\hat{K}_{\text{elastic}}$ for a particular plate under consideration in formula (4.3), a generalized form is obtained as

$$\hat{K}_{\text{plastic}} = 1 + (\hat{K}_{\text{elastic}} - 1)\frac{(E_s)_{\text{max stress}}}{(E_s)_\infty} \tag{4.6}$$

where the stress concentration is defined as $\hat{K} = (\hat{\sigma}_{\max})/\hat{\sigma}_\infty$. This relation includes the Hardrath–Ohman formula (4.5) for pure tension and is therefore proposed, tentatively, as a relation between $\hat{K}_{\text{plastic}}$ and $\hat{K}_{\text{elastic}}$ not only for a pure tension but also for a pure

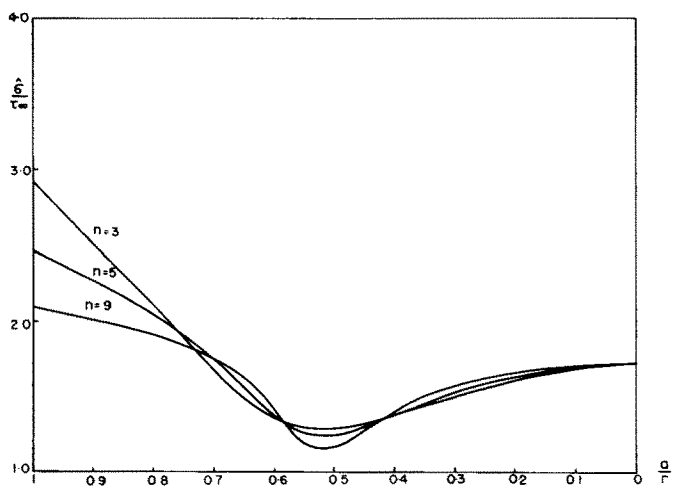

FIG. 17(b). Stress distribution of $\hat{\sigma}$ along $\theta = \pi/4$ for $\lambda = 0{\cdot}7$.

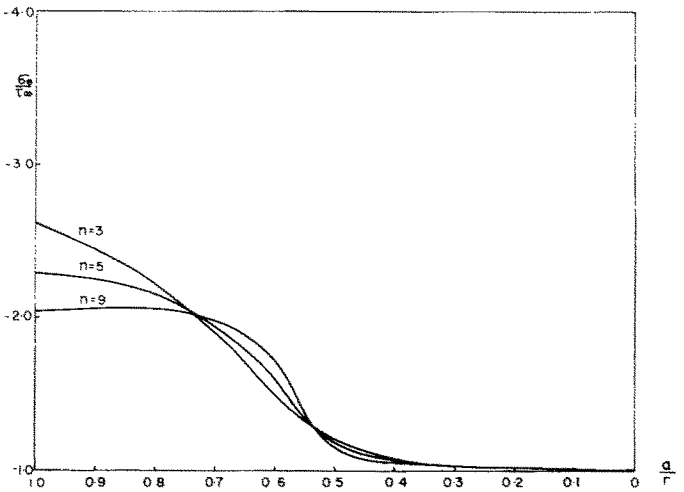

FIG. 18(a). Stress distribution of σ_θ along $\theta = \pi/4$ for $\lambda = \infty$.

shear plate with arbitrary holes, notches or fillets. Furthermore, it appears that this formula may be applicable to other stress states. A test for the case of balanced biaxial tension plate with a circular hole is shown in Table 6. Here the stress concentration factor K defined as $K = [(\sigma_\theta)_{\text{hole}}]/\sigma_\infty$ is found from the equation

$$K = 1 + \frac{1 + \frac{3}{7}\lambda^{n-1}}{1 + \frac{3}{7}\lambda^{n-1}K^{n-1}} \tag{4.7}$$

obtained from formula (4.6) with the use of the Ramberg–Osgood relation. It is seen that the agreement with the results obtained by Budiansky and Mangasarian [2] is fairly good.

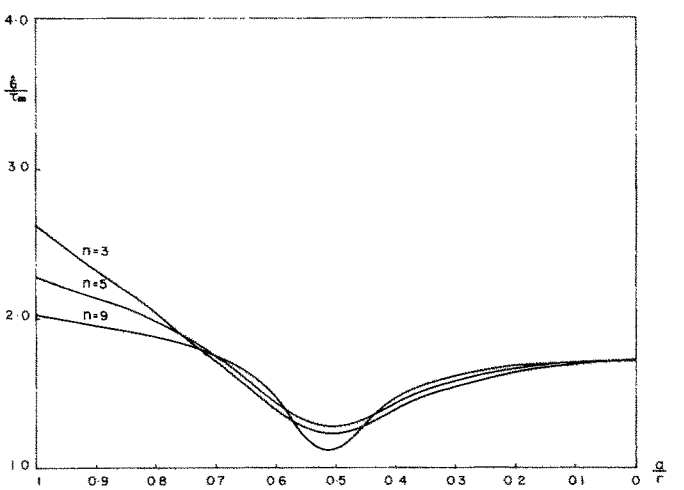

FIG. 18(b). Stress distribution of $\hat{\sigma}$ along $\theta = \pi/4$ for $\lambda = \infty$.

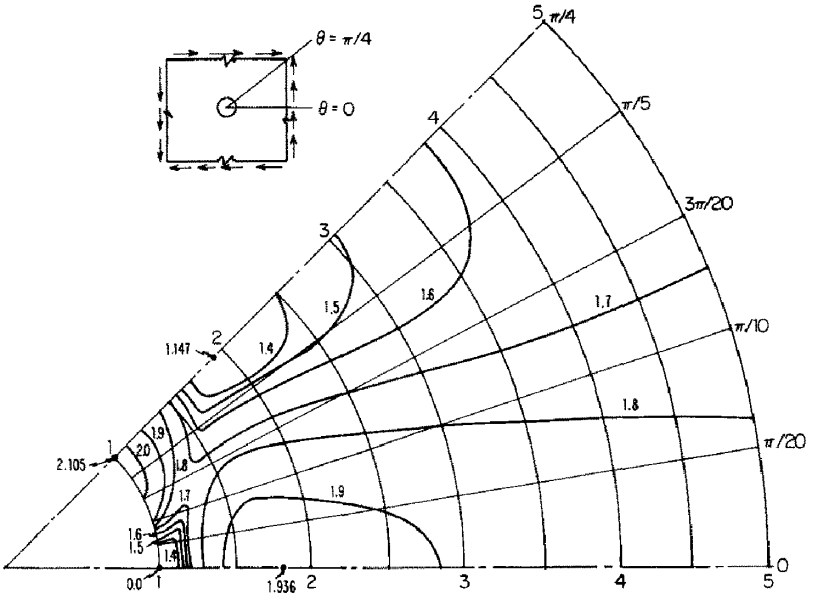

FIG. 19(a). Effective stress distributions for $\lambda = 0{\cdot}7$ and $n = 9$.

On Neuber's rule

By considering a notched prismatic body, obeying an arbitrary non-linear stress–strain law, and subjected to antiplane shear, Neuber [11] derived a relationship between stress and strain concentration factors as

$$K_\sigma K_\varepsilon = K_H^2 \tag{4.8}$$

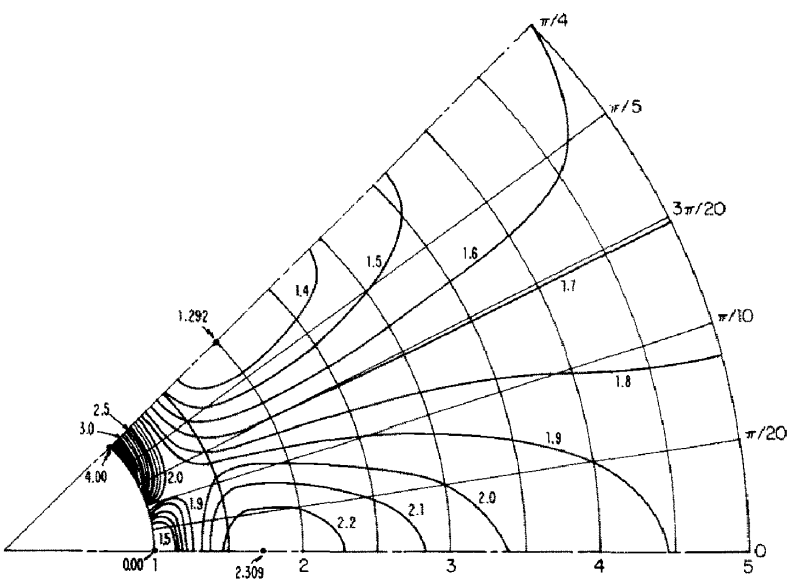

FIG. 19(b). Effective stress distributions in the elastic range.

TABLE 3. STRESS DISTRIBUTIONS IN A PURE SHEAR PLATE FOR $n = 9$ AND $\lambda = 0{\cdot}7$

a/r \ θ	0	$\pi/20$	$\pi/10$	$3\pi/20$	$\pi/5$	$\pi/4$
(a) S_r						
0·0	0·000	0·309	0·588	0·809	0·951	1·000
0·1	0·000	0·208	0·496	0·758	0·917	0·972
0·2	0·000	0·121	0·311	0·608	0·826	0·892
0·3	0·000	0·095	0·190	0·385	0·654	0·759
0·4	0·000	0·090	0·149	0·209	0·380	0·520
0·5	0·000	0·098	0·140	0·134	0·088	0·049
0·6	0·000	0·114	0·143	0·114	−0·164	−0·550
0·7	0·000	0·122	0·157	−0·019	−0·429	−0·605
0·8	0·000	0·124	0·055	−0·243	−0·384	−0·413
0·9	0·000	0·034	−0·098	−0·184	−0·202	−0·212
1·0	0·000	0·000	0·000	0·000	0·000	0·000
(b) S_θ						
0·0	0·000	−0·309	−0·588	−0·809	−0·951	−1·000
0·1	0·000	−0·312	−0·592	−0·813	−0·956	−1·005
0·2	0·000	−0·321	−0·610	−0·832	−0·972	−1·021
0·3	0·000	−0·329	−0·631	−0·864	−0·998	−1·043
0·4	0·000	−0·335	−0·646	−0·899	−1·040	−1·070
0·5	0·000	−0·341	−0·659	−0·931	−1·104	−1·144
0·6	0·000	−0·350	−0·690	−0·990	−1·341	−1·618
0·7	0·000	−0·391	−0·776	−1·289	−1·859	−2·000
0·8	0·000	−0·491	−1·149	−1·862	−2·072	−2·093
0·9	0·000	−0·924	−1·742	−2·045	−2·112	−2·120
1·0	0·000	−1·386	−1·910	−2·059	−2·097	−2·105
(c) $S_{r\theta}$						
0·0	1·000	0·951	0·809	0·588	0·309	0·000
0·1	1·032	0·982	0·831	0·599	0·314	0·000
0·2	1·066	1·025	0·886	0·637	0·329	0·000
0·3	1·089	1·053	0·939	0·709	0·366	0·000
0·4	1·103	1·072	0·970	0·784	0·447	0·000
0·5	1·114	1·082	0·993	0·829	0·560	0·000
0·6	1·114	1·087	0·994	0·839	0·520	0·000
0·7	1·098	1·060	0·953	0·657	0·159	0·000
0·8	1·013	0·965	0·688	0·227	0·033	0·000
0·9	0·774	0·590	0·232	0·058	0·012	0·000
1·0	0·000	0·000	0·000	0·000	0·000	0·000
(d) $\hat{S}$						
0·0	1·732	1·732	1·732	1·732	1·732	1·732
0·1	1·788	1·761	1·721	1·712	1·711	1·711
0·2	1·847	1·819	1·736	1·668	1·660	1·658
0·3	1·886	1·864	1·788	1·653	1·574	1·567
0·4	1·910	1·897	1·833	1·698	1·490	1·405
0·5	1·930	1·915	1·872	1·752	1·504	1·169
0·6	1·930	1·929	1·887	1·794	1·554	1·425
0·7	1·903	1·893	1·863	1·713	1·708	1·777
0·8	1·755	1·764	1·675	1·797	1·910	1·920
0·9	1·340	1·389	1·742	1·962	2·019	2·023
1·0	0·000	1·386	1·910	2·059	2·097	2·105

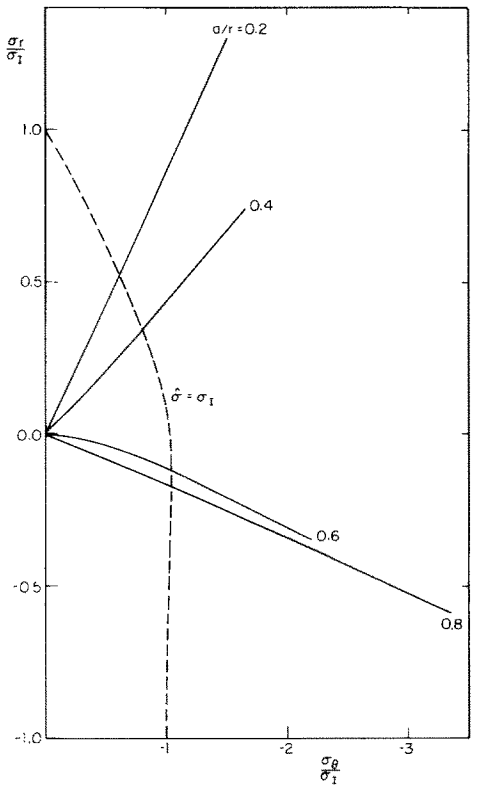

FIG. 20. Stress history at fixed points along $\theta = \pi/4$ for $n = 3$.

where K_σ and K_ε are the stress and strain concentration factor, respectively, and K_H is the elastic stress (or strain) concentration factor.

Neuber suggested that this rule may be applicable to other stress states. It is interesting to examine the validity of this rule for plane stress problems on the basis of the results obtained in the last section.

Figures 22 and 23 show plots of $K_\sigma K_\varepsilon / K_H^2$ vs. λ for a pure tension plate and a pure shear plate with a circular hole, respectively, as given by the present results. Since the stress state at the hole is uniaxial, the values of K_ε are directly calculated from the Ramberg–Osgood relation as

$$K_\varepsilon = \frac{(\varepsilon_\theta)_{a,\pi/2}}{\varepsilon_\infty} = \frac{K_\sigma(1 + \frac{3}{7}\lambda^{n-1}K_\sigma^{n-1})}{1 + \frac{3}{7}\lambda^{n-1}} \qquad \text{for pure tension}$$

and

$$K_\varepsilon = \frac{(\varepsilon_\theta)_{a,\pi/4}}{\varepsilon_\infty} = \frac{K_\sigma(1 + \frac{3}{7}\lambda^{n-1}K_\sigma^{n-1})}{1 + \frac{3}{7}\sqrt{(3)^{(n-1)}}\lambda^{n-1}} \qquad \text{for pure shear.}$$

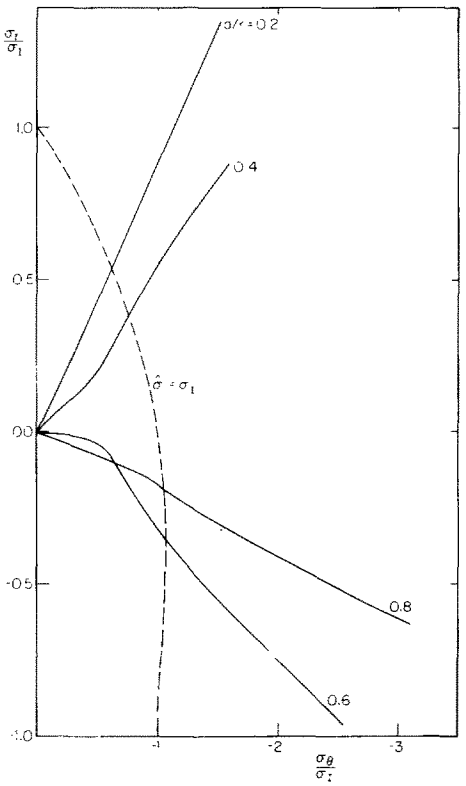

FIG. 21. Stress history at fixed points along $\theta = \pi/4$ for $n = 9$.

TABLE 4. STRESS CONCENTRATION FACTORS IN A PURE TENSION PLATE

		K		
	λ	Stowell	Present ($M = 4$)	Neuber
	0·3	2·63	2·65	2·70
	0·5	2·38	2·40	2·51
$n = 3$	0·8	2·11	2·17	2·21
	1·5	1·89	1·94	1·95
	∞	1·76	1·80	1·73
			($M = 5$)	
	0·8	2·69	2·68	2·75
	0·5	2·24	2·24	2·30
$n = 5$	0·8	1·82	1·85	1·86
	1·5	1·52	1·59	1·55
	∞	1·46	1·52	1·44
			($M = 6$)	
	0·3	2·80	2·79	2·82
	0·5	2·14	2·13	2·19
$n = 9$	0·8	1·58	1·58	1·59
	1·5	1·29	1·30	1·26
	∞	1·28	1·29	1·25

TABLE 5. STRESS CONCENTRATION FACTORS IN A PURE SHEAR PLATE

		K		
	λ	Formula (4.4)	Present ($M = 3$)	Neuber
$n = 3$	0·2	−3·66	−3·62	−3·69
	0·4	−3·22	−3·22	−3·31
	0·7	−3·00	−2·93	−3·00
	1·0	−2·87	−2·80	−2·85
	1·5	−2·77	−2·71	−2·74
	∝	−2·67	−2·62	−2·63
			($M = 4$)	
$n = 5$	0·2	−3·74	−3·69	−3·76
	0·4	−2·96	−2·93	−3·04
	0·7	−2·52	−2·46	−2·49
	1·0	−2·42	−2·34	−2·35
	1·5	−2·38	−2·30	−2·31
	∞	−2·37	−2·30	−2·29
			($M = 5$)	
$n = 9$	0·2	−3·88	−3·85	−3·89
	0·4	−2·82	−2·73	−2·75
	0·7	−2·20	−2·11	−2·12
	1·0	−2·15	−2·06	−2·05
	1·5	−2·14	−2·05	−2·04
	∞	−2·14	−2·05	−2·04

TABLE 6. STRESS CONCENTRATION FACTOR IN A BALANCED BIAXIAL TENSION PLATE

		K		
	λ	Formula (4.7)	Budiansky and Mangasarian	Neuber
$n = 3$	0·4	1·86	1·82	1·86
	0·8	1·70	1·64	1·69
	1·0	1·65	1·57	1·63
	1·5	1·57	1·44	1·54
	∞	1·46	1·36	1·41
$n = 5$	0·4	1·88	1·85	1·88
	0·8	1·56	1·49	1·54
	1·0	1·47	1·38	1·43
	1·5	1·37	1·23	1·31
	∞	1·32	1·22	1·26
$n = 9$	0·4	1·95	1·94	1·95
	0·8	1·45	1·38	1·42
	1·0	1·30	1·22	1·26
	1·5	1·21	1·12	1·15
	∞	1·21	1·12	1·15

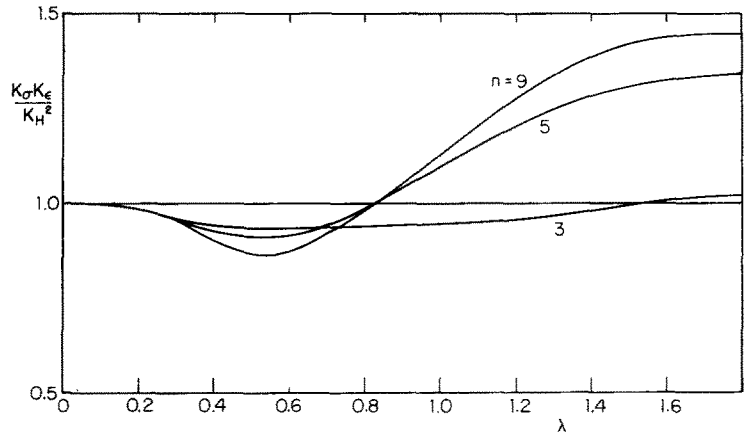

FIG. 22. Curves of $K_\sigma K_\varepsilon / K_H^2$ with λ in a pure tension plate.

Without reference to the present analysis, the stress concentration factor K_σ can be found directly from the equations

$$K_\sigma^2 = \frac{9(1+\frac{3}{7}\lambda^{n-1})}{1+\frac{3}{7}\lambda^{n-1}K_\sigma^{n-1}} \qquad \text{for pure tension}$$

and

$$K_\sigma^2 = \frac{16(1+\frac{3}{7}\sqrt{(3)}^{(n-1)}\lambda^{n-1})}{1+\frac{3}{7}\lambda^{n-1}K_\sigma^{n-1}} \qquad \text{for pure shear}$$

obtained from the Neuber rule (4.8) with the use of the Ramberg–Osgood relation. These equations provide the values of K_σ (by trial and error) shown in Tables 4 and 5.

It is seen that Neuber's rule gives a slightly higher value of the stress concentration factor than that obtained from the present numerical analysis when the strain is small, and gives a slightly lower value when the strain is large. The difference is smaller for the

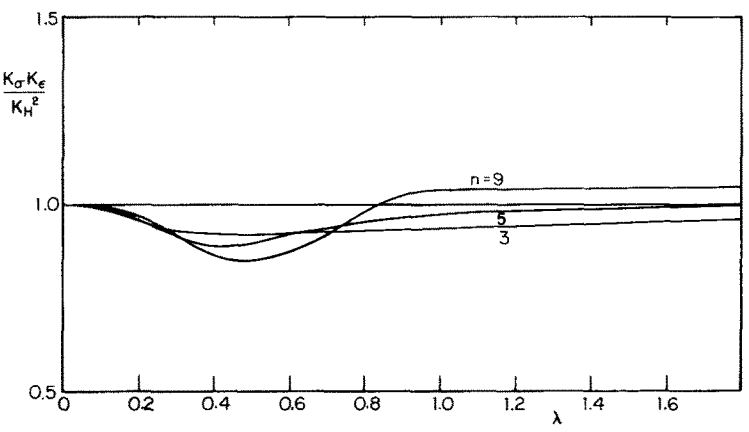

FIG. 23. Curves of $K_\sigma K_\varepsilon / K_H^2$ with λ in a pure shear plate.

case of pure shear than for the case of pure tension. Generally speaking, this rule gives an accurate result for the stress concentration factor. It should be noted that in Fig. 22 the considerably large deviations from the Neuber rule for λ and n large are associated with very small differences between the stress concentration factors predicted by the Neuber rule and the present analysis. The reason is that small increases of stress can produce very large strain differences when n is not small. Thus, the use of plots like those in Fig. 22 to assess how well experimental data follow the Neuber rule might be somewhat misleading.

A further test for the case of balanced biaxial tension plate with a circular hole is shown in Table 6 where the stress concentration factor K_σ is given by

$$K_\sigma^2 = \frac{4(1+\frac{3}{7}\lambda^{n-1})}{1+\frac{3}{7}\lambda^{n-1}K_\sigma^{n-1}}.$$

This is obtained from the Neuber rule (4.8) with the use of the Ramberg–Osgood relation. It is seen that the Neuber rule gives a result between those obtained from formula (4.6) and by Budiansky and Mangasarian.

5. STRESS DISTRIBUTION AROUND A RIGID CIRCULAR CYLINDRICAL INCLUSION IN AN INFINITE MATRIX SUBJECTED TO TRANSVERSE LOADING

An infinitely long cylindrical inclusion in a matrix under transverse pure shear

(a) *Governing equation and boundary conditions.* As shown in Fig. 3, the uniform load applied at infinity is perpendicular to the cylindrical direction, and therefore the body may be assumed to be in a condition of plane strain. Since the inclusion is rigid, the strain components in the longitudinal direction vanish, i.e. $\varepsilon_z = 0$. Hence the stress function is governed by equation (2.11) in a power law strain hardening matrix.

On the boundary of the rigid inclusion

$$U(1) = V(1) = 0.$$

These give the boundary conditions

$$\varepsilon_\theta(1) = 0, \quad \text{whence} \quad F''(1) - F'(1) - F^{\cdot\cdot}(1) = 0 \tag{5.1}$$

and

$$2\varepsilon_{r\theta}^{\cdot}(1) + \varepsilon_\theta'(1) = 0$$

which leads to

$$F'''(1) + [3+4(n-1)]F^{\cdot\cdot\cdot}(1) - [3+4(n-1)]F^{\cdot\cdot}(1) = 0. \tag{5.2}$$

For pure shear loading at infinity, the boundary conditions at $x = 0$ are

$$\begin{aligned} F(0) &= -\tfrac{1}{2}\sin 2\theta \\ F'(0) &= 0 \end{aligned} \tag{5.3}$$

and the modified stress function has the form

$$F = \sum_{m=2,6,10,\ldots} f_m(x)\sin m\theta.$$

(b) *Results and discussion.* By the method presented in Section 2, equation (2.11) and boundary conditions (5.1)–(5.3) were solved for the values of $n = 3, 5, 7$. Depending on n, three to five terms in the fourier series were needed for satisfactory convergence as measured by a difference of the result for the maximum stress less than 1 per cent when an additional term was added.

Table 7 shows the stress distributions of all the stress components for $n = 7$. It is seen that the circumferential stress component σ_θ has a very sharp gradient at the points immediately away from the inclusion, and the maximum effective stress is at $\theta = 0$, $r = a$. The spatial stress distributions of σ_r along $\theta = \pi/4$ and $\hat{\sigma}$ along $\theta = 0$ for $n = 3, 5, 7$ are shown in Figs. 24(a) and (b).

An application of these results to the theory of fiber reinforced materials is given in Ref. [15].

An infinitely long cylindrical inclusion in a matrix under transverse pure tension

For problems under plane strain conditions with $\varepsilon_z = 0$ in an incompressible material, the solution for the case under pure tension (see Fig. 4) can be obtained by superposing the solution for the pure shear case and the solution for the balanced biaxial tension case as shown below:

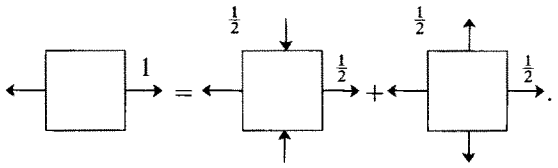

In the balanced biaxial tension case, incompressibility forces the stresses to be constant and the strains to vanish everywhere. The effective stress at each point in the pure tension body is the same as that at the corresponding point in the pure shear body. Therefore, if the stresses in the pure shear case with loading $S_{r\theta} = 1$ at $\theta = 0$ are

$$S_r = \sum S_{rm}(x) \sin m\theta$$

$$S_\theta = \sum S_{\theta m}(x) \sin m\theta$$

$$S_{r\theta} = \sum S_{r\theta m}(x) \cos m\theta$$

the solution for the case under pure tension with loading $S_r = 1$ at $\theta = 0$ is

$$S_r = \tfrac{1}{2}[1 + \sum S_{rm}(x) \sin m(\theta + \pi/4)]$$

$$S_\theta = \tfrac{1}{2}[1 + \sum S_{\theta m}(x) \sin m(\theta + \pi/4)]$$

$$S_{r\theta} = \tfrac{1}{2} \sum S_{r\theta}(x) \cos m(\theta + \pi/4).$$

Table 8 shows the stress distributions of all the stress components for $n = 7$. It is worthy of note that the effective stress is symmetric with respect to $\theta = \pi/4$ and attains its maximum at $\theta = \pi/4$, $r = a$.

TABLE 7. STRESS DISTRIBUTIONS AROUND A CYLINDRICAL INCLUSION UNDER TRANSVERSE PURE SHEAR FOR $n = 7$

a/r \ θ	0	$\pi/28$	$\pi/14$	$3\pi/28$	$\pi/7$	$5\pi/28$	$3\pi/14$	$\pi/4$
(a) S_r								
0·0	0·000	0·223	0·433	0·623	0·781	0·901	0·975	1·000
0·1	0·000	0·252	0·465	0·638	0·787	0·906	0·979	1·001
0·2	0·000	0·318	0·546	0·692	0·815	0·924	0·991	1·010
0·3	0·000	0·365	0·631	0·786	0·884	0·962	1·018	1·038
0·4	0·000	0·366	0·675	0·882	0·989	1·040	1·072	1·086
0·5	0·000	0·349	0·668	0·923	1·086	1·158	1·170	1·167
0·6	0·000	0·343	0·645	0·906	1·125	1·265	1·312	1·315
0·7	0·000	0·336	0·635	0·888	1·110	1·308	1·458	1·516
0·8	0·000	0·327	0·636	0·896	1·111	1·327	1·531	1·620
0·9	0·000	0·343	0·641	0·912	1·173	1·371	1·462	1·480
1·0	0·000	0·361	0·636	0·903	1·188	1·316	1·221	1·130
(b) S_θ								
0·0	0·000	−0·223	−0·433	−0·623	−0·781	−0·901	−0·975	−1·000
0·1	0·000	−0·222	−0·434	−0·624	−0·782	−0·901	−0·975	−1·000
0·2	0·000	−0·221	−0·432	−0·623	−0·783	−0·903	−0·977	−1·003
0·3	0·000	−0·215	−0·423	−0·614	−0·777	−0·900	−0·976	−1·001
0·4	0·000	−0·209	−0·407	−0·589	−0·751	−0·880	−0·960	−0·987
0·5	0·000	−0·206	−0·393	−0·557	−0·702	−0·826	−0·914	−0·946
0·6	0·000	−0·201	−0·387	−0·538	−0·648	−0·737	−0·812	−0·844
0·7	0·000	−0·196	−0·378	−0·526	−0·619	−0·653	−0·650	−0·643
0·8	0·000	−0·192	−0·353	−0·482	−0·562	−0·543	−0·444	−0·385
0·9	0·000	−0·143	−0·248	−0·294	−0·273	−0·200	−0·115	−0·077
1·0	0·000	0·361	0·636	0·903	1·188	1·316	1·221	1·130
(c) $S_{r\theta}$								
0·0	1·000	0·975	0·901	0·781	0·623	0·433	0·223	0·000
0·1	0·990	0·966	0·896	0·779	0·622	0·433	0·222	0·000
0·2	0·965	0·942	0·874	0·764	0·614	0·429	0·220	0·000
0·3	0·944	0·914	0·837	0·729	0·590	0·417	0·214	0·000
0·4	0·937	0·899	0·804	0·680	0·542	0·385	0·202	0·000
0·5	0·934	0·899	0·797	0·646	0·483	0·329	0·172	0·000
0·6	0·938	0·907	0·811	0·654	0·462	0·275	0·122	0·000
0·7	0·957	0·920	0·827	0·691	0·503	0·288	0·112	0·000
0·8	0·977	0·948	0·864	0·736	0·585	0·419	0·224	0·000
0·9	1·017	1·008	0·951	0·842	0·740	0·637	0·404	0·000
1.0	1·274	1·256	1·205	1·124	1·007	0·807	0·465	0·000
(d) $\hat{S}/\sqrt{3}$								
0·0	1·000	1·000	1·000	1·000	1·000	1·000	1·000	1·000
0·1	0·990	0·995	1·002	1·002	1·001	1·002	1·002	1·001
0·2	0·965	0·980	1·002	1·008	1·008	1·009	1·008	1·007
0·3	0·944	0·959	0·989	1·011	1·019	1·020	1·020	1·019
0·4	0·937	0·944	0·969	1·002	1·025	1·034	1·036	1·037
0·5	0·934	0·941	0·958	0·983	1·016	1·045	1·056	1·056
0·6	0·938	0·947	0·961	0·974	1·000	1·038	1·068	1·079
0·7	0·957	0·958	0·970	0·988	1·000	1·022	1·060	1·079
0·8	0·977	0·983	0·995	1·008	1·021	1·025	1·012	1·002
0·9	1·017	1·036	1·050	1·036	1·035	1·011	0·886	0·779
1·0	1·274	1·256	1·205	1·124	1·007	0·807	0·465	0·000

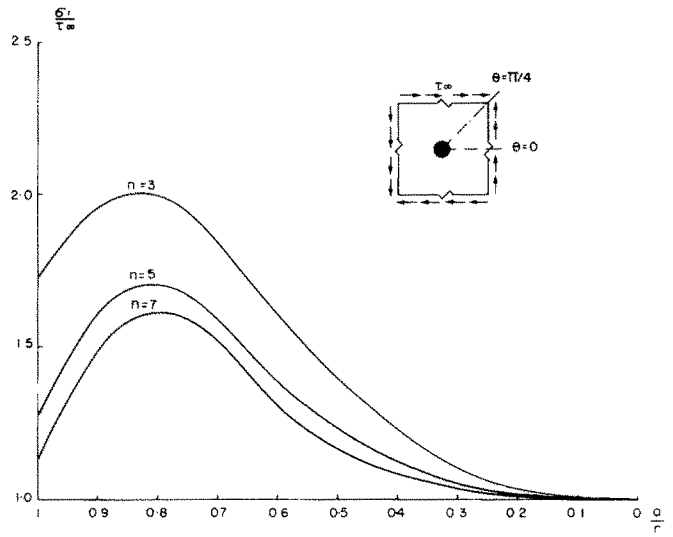

FIG. 24(a). Stress distribution of σ_y along $\theta = \pi/4$.

6. THE APPLICABILITY OF THE POWER LAW SOLUTION TO STEADY CREEP

For the metals used in structures, the experimentally established steady creep law is often taken in the form

$$\dot{\varepsilon} = k\sigma^n \tag{6.1}$$

where $\dot{\varepsilon}$ is the tensile strain rate caused by uniaxial tension σ and k, n are constants obtained from constant temperature creep tests.

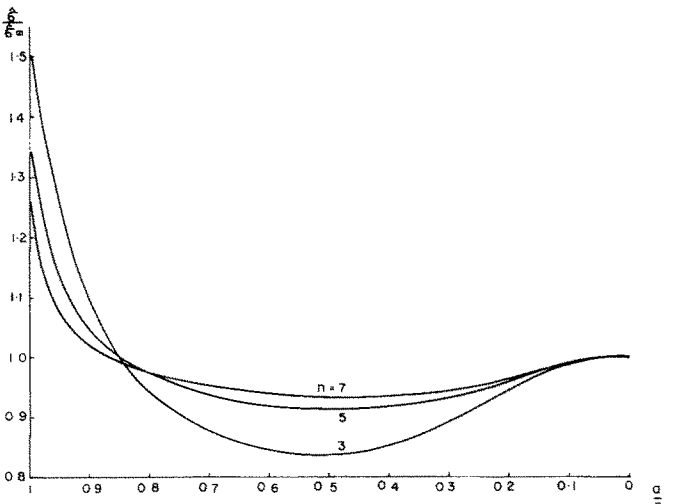

FIG. 24(b). Stress distribution of $\hat{\sigma}$ along $\theta = 0$.

TABLE 8. STRESS DISTRIBUTIONS AROUND A CYLINDRICAL INCLUSION UNDER TRANSVERSE PURE TENSION FOR $n = 7$

a/r \ θ	0	$\pi/20$	$\pi/10$	$3\pi/20$	$\pi/5$	$\pi/4$	$3\pi/10$	$7\pi/20$	$2\pi/5$	$9\pi/20$	$\pi/2$
(a) S_r											
0·0	1·000	0·976	0·905	0·794	0·655	0·500	0·346	0·206	0·096	0·025	0·000
0·1	1·001	0·978	0·907	0·803	0·672	0·500	0·328	0·197	0·093	0·022	−0·001
0·2	1·005	0·985	0·919	0·833	0·711	0·500	0·289	0·167	0·081	0·015	−0·005
0·3	1·019	1·000	0·951	0·881	0·743	0·500	0·257	0·119	0·049	0·000	−0·019
0·4	1·043	1·030	1·001	0·925	0·750	0·500	0·250	0·075	−0·001	−0·030	−0·043
0·5	1·084	1·085	1·054	0·939	0·741	0·500	0·259	0·061	−0·054	−0·085	−0·084
0·6	1·157	1·151	1·080	0·928	0·735	0·500	0·265	0·072	−0·080	−0·151	−0·157
0·7	1·258	1·203	1·076	0·920	0·731	0·500	0·269	0·080	−0·076	−0·203	−0·258
0·8	1·310	1·228	1·077	0·924	0·728	0·500	0·273	0·076	−0·077	−0·228	−0·310
0·9	1·240	1·219	1·110	0·929	0·734	0·500	0·266	0·071	−0·110	−0·219	−0·240
1·0	1·065	1·138	1·116	0·923	0·740	0·500	0·260	0·077	−0·116	−0·138	−0·065
(b) S_θ											
0·0	0·000	0·025	0·096	0·206	0·346	0·500	0·655	0·794	0·905	0·976	1·000
0·1	0·000	0·024	0·095	0·206	0·346	0·500	0·654	0·794	0·905	0·976	1·000
0·2	−0·001	0·023	0·095	0·206	0·346	0·500	0·654	0·794	0·905	0·977	1·001
0·3	−0·001	0·024	0·098	0·211	0·350	0·500	0·650	0·789	0·902	0·976	1·001
0·4	0·007	0·033	0·110	0·223	0·355	0·500	0·645	0·777	0·890	0·977	0·993
0·5	0·027	0·058	0·136	0·237	0·358	0·500	0·642	0·763	0·864	0·942	0·973
0·6	0·078	0·107	0·167	0·244	0·361	0·500	0·639	0·756	0·833	0·893	0·922
0·7	0·178	0·174	0·185	0·250	0·364	0·500	0·636	0·750	0·815	0·826	0·822
0·8	0·308	0·257	0·216	0·271	0·370	0·500	0·630	0·729	0·784	0·743	0·692
0·9	0·461	0·427	0·369	0·355	0·404	0·500	0·596	0·645	0·631	0·573	0·539
1·0	1·065	1·138	1·116	0·923	0·740	0·500	0·260	0·077	−0·116	−0·138	−0·065
(c) $S_{r\theta}$											
0·0	0·000	−0·155	−0·294	−0·405	−0·476	−0·500	−0·476	−0·405	−0·294	−0·155	0·000
0·1	0·000	−0·154	−0·293	−0·403	−0·472	−0·495	−0·472	−0·403	−0·293	−0·154	0·000
0·2	0·000	−0·153	−0·290	−0·395	−0·460	−0·482	−0·460	−0·395	−0·290	−0·153	0·000
0·3	0·000	−0·149	−0·280	−0·376	−0·444	−0·472	−0·444	−0·376	−0·279	−0·149	0·000
0·4	0·000	−0·139	−0·256	−0·353	−0·433	−0·468	−0·433	−0·353	−0·256	−0·139	0·000
0·5	0·000	−0·118	−0·226	−0·339	−0·433	−0·467	−0·433	−0·339	−0·226	−0·118	0·000
0·6	0·000	−0·089	−0·211	−0·345	−0·438	−0·469	−0·438	−0·345	−0·211	−0·089	0·000
0·7	0·000	−0·087	−0·230	−0·361	−0·444	−0·478	−0·444	−0·361	−0·230	−0·087	0·000
0·8	0·000	−0·153	−0·277	−0·382	−0·460	−0·489	−0·460	−0·382	−0·277	−0·153	0·000
0·9	0·000	−0·260	−0·361	−0·433	−0·496	−0·508	−0·496	−0·433	−0·361	−0·260	0·000
1·0	0·000	−0·310	−0·488	−0·571	−0·620	−0·637	−0·620	−0·571	−0·488	−0·310	0·000
(d) $\hat{S}/\sqrt{3}$											
0·0	0·500	0·500	0·500	0·500	0·500	0·500	0·500	0·500	0·500	0·500	0·500
0·1	0·500	0·501	0·501	0·501	0·499	0·495	0·499	0·501	0·501	0·501	0·500
0·2	0·503	0·505	0·504	0·504	0·495	0·482	0·495	0·504	0·504	0·505	0·503
0·3	0·510	0·510	0·510	0·504	0·486	0·472	0·486	0·504	0·510	0·510	0·510
0·4	0·518	0·518	0·514	0·498	0·476	0·468	0·476	0·498	0·514	0·518	0·518
0·5	0·528	0·527	0·512	0·488	0·474	0·467	0·474	0·488	0·512	0·527	0·528
0·6	0·540	0·529	0·503	0·486	0·476	0·469	0·476	0·486	0·503	0·529	0·540
0·7	0·540	0·522	0·501	0·493	0·481	0·478	0·481	0·493	0·501	0·522	0·540
0·8	0·501	0·509	0·512	0·503	0·494	0·489	0·494	0·503	0·512	0·509	0·501
0·9	0·389	0·474	0·518	0·519	0·523	0·508	0·523	0·519	0·518	0·474	0·389
1·0	0·000	0·310	0·488	0·571	0·620	0·637	0·620	0·571	0·488	0·310	0·000

The generalized steady creep law for polyaxial stresses proposed by Odqvist [16] which reduces to (6.1) in simple tension is

$$\dot{\varepsilon}_{ij} = \tfrac{3}{2}k\hat{\sigma}^{n-1}S_{ij} \tag{6.2}$$

where $\dot{\varepsilon}_{ij}$ are strain rates, and S_{ij} are stress deviators defined as

$$S_{ij} = \sigma_{ij} - \tfrac{1}{3}\delta_{ij}\sigma_{kk}$$

and $\hat{\sigma}$ is the effective stress given by

$$\hat{\sigma} = \sqrt{(\tfrac{3}{2}S_{ij}S_{ij})}.$$

The analogy with the simple power-law deformation theory of plasticity is clear. Therefore, the solutions of the limiting case $\lambda = \infty$ presented in the previous sections also provide the steady creep solutions for the stresses in the corresponding problems.

7. CONCLUDING REMARKS

For an elastoplastic analysis of a plane problem with an infinite region exterior to a circular boundary, the present method involving fourier series and finite difference appears to be useful and accurate. Comparisons of numerical results show that the generalized Stowell formula presented in this paper and the Neuber rule provide reasonably accurate plastic stress concentration factors for plane stress problems under pure tension, pure shear and balanced biaxial tension. These two rules may also be applicable to other loading conditions.

REFERENCES

[1] M. H. LEE WU, Analysis of Plane-Stress Problems with Axial Symmetry in Strain Hardening Range, NACA TR 1021 (1951).
[2] B. BUDIANSKY and O. L. MANGASARIAN, Plastic stress concentration at a circular hole in an infinite sheet subjected to equal biaxial tension. *J. appl. Mech.* **27**, 59 (1960).
[3] I. S. TUBA, Elastic–plastic stress and strain concentration factors at a circular hole in a uniformly stressed infinite plate. *J. appl. Mech.* **32**, 710 (1965).
[4] I. S. TUBA, Notes on elastic–plastic analysis. *J. Franklin Inst.* **285** (1968).
[5] A. MENDELSON, Elastoplastic Analysis of Circular Cylindrical Inclusion in Uniformly Stressed Infinite Homogeneous Matrix, NASA TN D-4350 (1968).
[6] B. BUDIANSKY and R. J. VIDENSEK, Analysis of Stress in the Plastic Range Around a Circular Hole in a Plate Subjected to Uniaxial Tension, NACA TN 3542 (1955).
[7] I. S. TUBA, An analytic method for elastic–plastic solution. *Int. J. Solids Struct.* **3**, 543 (1967).
[8] P. V. MARCAL and I. P. KING, Elastic–plastic analysis of two-dimensional stress systems by the finite element method. *Int. J. Mech. Sci.* **9**, 143 (1967).
[9] E. Z. STOWELL, Stress and Strain Concentration at a Circular Hole in an Infinite Plate, NACA TN 2073 (1950).
[10] H. E. HARDRATH and L. OHMAN, A Study of Elastic and Plastic Stress Concentration Factors due to Notches and Fillets in Flat Plates, NACA TR 1117 (1953).
[11] H. NEUBER, Theory of stress concentration for shear-strained prismatical bodies with arbitrary nonlinear stress strain law. *J. appl. Mech.* **28**, 544 (1961).
[12] B. BUDIANSKY, A reassessment of deformation theories of plasticity. *J. appl. Mech.* **26**, 259 (1959).
[13] M. L. POTTERS, A Matrix Method for the Solution of a Second Order Difference Equation in Two Variables, Report MR 19, Mathematich Centrum, Amsterdam, Holland (1955).
[14] W. RAMBERG and W. R. OSGOOD, Description of Stress–Strain Curves by Three Parameters, NACA TN 902 (1943).
[15] W. C. HUANG, Plastic behavior of some composite materials. *J. Composite Mater.* **5** (1971).
[16] F. K. G. ODQVIST, Plasticitetsteori . . . , The Royal Swedish Institute of Engineering Research (1934); IV *International Congress for Applied Mechanics*, p. 78 (1934).

APPENDIX A

Potters' method

For the sake of completeness, a brief description of Potters' method [13] used in the present analysis will be given here.

Rewrite the set of fourth order linear differential equations (2.14) or (2.19) in the form

$$\sum_{m}^{M} (e^j_{4m} q''''_m + e^j_{3m} q'''_m + e^j_{2m} q''_m + e^j_{1m} q'_m + e^j_{0m} q_m) = r^j. \tag{A1}$$

Let $q''_m = p_m$ and with the use of the central difference formula (with equal mesh points, $i = 1, 2, 3, \ldots N$), equation (A1) can be written in the matrix form as

$$A_i y_{i-1} + B_i y_i + C_i y_{i+1} = R_i, \qquad i = 2, 3, \ldots N-1 \tag{A2}$$

where

$$y_i = \begin{bmatrix} p_{1i} \\ q_{1i} \\ p_{2i} \\ q_{2i} \\ \vdots \\ p_{Mi} \\ q_{Mi} \end{bmatrix}$$

R is a column vector and A, B, C are $2M \times 2M$ coefficient matrices. In the application of Potters' method, a vector P and a matrix Q are introduced by writing

$$y_i = P_i + Q_i y_{i+1}, \qquad i = 1, 2, 3, \ldots N. \tag{A3}$$

Substitution in (A2) leads to the recurrent relations

$$\begin{aligned} P_{i+1} &= (A_{i+1} Q_i + B_{i+1})^{-1} (R_{i+1} - A_{i+1} P_i) \\ Q_{i+1} &= -(A_{i+1} Q_i + B_{i+1})^{-1} C_{i+1} \\ i &= 1, 2, 3, \ldots N-1. \end{aligned} \tag{A4}$$

Similarly, write the boundary condition at $x = 1$ in the form

$$S y_{N-1} + T y_N + W y_{N+1} = k \tag{A5}$$

where S, T, W are again $2M \times 2M$ matrices and an $(N+1)$st mesh point has been introduced to permit a central difference representation of derivative on the boundary $x = 1$. With the use of (A3), the value of y for $(N+1)$st mesh point is

$$y_{N+1} = (S Q_{N-1} Q_N + T Q_N + W)^{-1} (k - S Q_{N-1} P_N - S P_{N-1} - T P_N) \tag{A6}$$

while the boundary conditions at $x = 0$ provides the knowledge of P_1 and Q_1. Thus, the equations are solved as follows:

First from (A4) we obtain P_i, Q_i for $i = 2, 3, \ldots N$ and y_{N+1} is calculated by (A6). Then by using (A3) we obtain y_i for $i = 1, 2, 3, \ldots N$.

APPENDIX B

Coefficients of equations (2.13) *and* (2.17)

(a) *Plane stress.* The d's in equation (2.17) are

$$d_1 = 2c_1x^4 + x^2H_3(2S_\theta - S_r)$$

$$d_2 = 4c_1x^3 + 4c_3x^4 + x^2H_2(2S_\theta - S_r) + x^2H_6(2S_\theta^{\cdot} - S_r^{\cdot}) + xH_3(-4S_r + 4xS_\theta' + 5S_\theta - 2xS_r')$$

$$d_3 = 6xH_3S_{r\theta} + x^2H_6(2S_\theta - S_r)$$

$$\begin{aligned} d_4 = {} & -2c_1x^2 + 2c_2x^4 + c_3x^3 - c_5x^2 + x^2H_1(2S_\theta - S_r) + xH_2(-2S_r + 2xS_\theta' + S_\theta - xS_r') \\ & + x^2H_4(2S_\theta^{\cdot} - S_r^{\cdot}) + xH_3(-4S_r' + 2xS_\theta'' + 2S_\theta' - xS_r'') + x^2H_5(2S_\theta^{\cdot\cdot} - S_r^{\cdot\cdot}) \\ & + xH_6(-2S_r^{\cdot} + 2xS_\theta^{\cdot\cdot} - xS_r^{\cdot\cdot} + S_\theta^{\cdot}) \end{aligned}$$

$$\begin{aligned} d_5 = {} & 4c_4x^2 + 6xH_2S_{r\theta} + x^2H_4(2S_\theta - S_r) + 6H_3(S_{r\theta} + 2xS_{r\theta}') + x^2H_5(4S_\theta^{\cdot} - 2S_r^{\cdot}) \\ & + xH_6(-2S_r + 2xS_\theta' + S_\theta - xS_r' + 6S_{r\theta}^{\cdot}) \end{aligned}$$

$$d_6 = 4c_1x^2 + H_3(2S_r - S_\theta) + x^2H_5(2S_\theta - S_r) + 6xH_6S_{r\theta}$$

$$\begin{aligned} d_7 = {} & 2c_1x - 3c_2x^3 - 2c_3x^2 - 3xH_1S_\theta + H_2(2S_r - S_\theta - 3xS_\theta') - 3xH_4S_\theta^{\cdot} - 3xH_5S_\theta^{\cdot\cdot} \\ & + H_3(4S_r' - 3xS_\theta'' - 2S_\theta') + H_6(2S_r^{\cdot} - 3xS_\theta^{\cdot\cdot} - S_\theta^{\cdot}) \end{aligned}$$

$$\begin{aligned} d_8 = {} & -6c_4x + 6c_6x^2 + 6S_{r\theta}xH_1 + 6xS_{r\theta}'H_2 + 6xS_{r\theta}''H_3 + xH_4(6S_{r\theta}^{\cdot} - 3S_\theta) \\ & + xH_5(6S_{r\theta}^{\cdot\cdot} - 6S_\theta^{\cdot}) + H_6(2S_r - 3xS_\theta' - S_\theta + 6xS_{r\theta}^{\cdot}) \end{aligned}$$

$$\begin{aligned} d_9 = {} & -4c_1x + 4c_3x^2 + H_2(2S_r - S_\theta) + 6xS_{r\theta}H_4 + H_3(4S_r' - 2S_\theta') \\ & + xH_5(12S_{r\theta}^{\cdot} - 3S_\theta) + H_6(2S_r^{\cdot} - S_\theta^{\cdot} + 6xS_{r\theta}') \end{aligned}$$

$$d_{10} = 6xH_5S_{r\theta} + H_6(2S_r - S_\theta)$$

$$\begin{aligned} d_{11} = {} & 2c_2x^2 + 2c_3x + 2c_5 + 2H_1(S_r + S_\theta) + 2H_2(S_r' + S_\theta') + 2H_4(S_r^{\cdot} + S_\theta^{\cdot}) + 2H_3(S_r'' + S_\theta'') \\ & + 2H_5(S_r^{\cdot\cdot} + S_\theta^{\cdot\cdot}) + 2H_6(S_r^{\cdot\cdot} + S_\theta^{\cdot\cdot}) \end{aligned}$$

$$\begin{aligned} d_{12} = {} & 10c_4 - 6c_6x - 6S_{r\theta}H_1 - 6S_{r\theta}'H_2 + 2H_4(S_r + S_\theta - 3S_{r\theta}^{\cdot}) \\ & - 6S_{r\theta}''H_3 + H_5(4S_r^{\cdot} + 4S_\theta^{\cdot} - 6S_{r\theta}^{\cdot\cdot}) + 2H_6(S_r' + S_\theta' - 3S_{r\theta}^{\cdot\cdot}) \end{aligned}$$

$$\begin{aligned} d_{13} = {} & 8c_1 - c_2x^2 - 4c_3x + 2c_5 + H_1(2S_r - S_\theta) + H_2(2S_r' - S_\theta') + H_4(2S_r^{\cdot} - S_\theta^{\cdot} - 6S_{r\theta}) \\ & + H_3(2S_r'' - S_\theta'') + H_6(2S_r^{\cdot\cdot} - S_\theta^{\cdot\cdot} - 6S_{r\theta}') + H_5(2S_r + 2S_r^{\cdot\cdot} + 2S_\theta - S_\theta^{\cdot\cdot} - 12S_{r\theta}^{\cdot}) \end{aligned}$$

$$d_{14} = 4c_4 + H_4(2S_r - S_\theta) + H_5(4S_r^{\cdot} - 2S_\theta^{\cdot} - 6S_{r\theta}) + H_6(2S_r' - S_\theta')$$

$$d_{15} = 2c_1 + H_5(2S_r - S_\theta)$$

where for λ finite

$$\begin{aligned} H_1 = {} & \tfrac{1}{2}(n-1)p[\tfrac{1}{2}(n-3)\tfrac{1}{2}(n-5)\mathfrak{S}^{\frac{1}{2}(n-7)}\mathfrak{S}'^{2}L_2 + \tfrac{1}{2}(n-3)\mathfrak{S}^{\frac{1}{2}(n-5)}\mathfrak{S}''L_2 + \tfrac{1}{2}(n-3)\mathfrak{S}^{\frac{1}{2}(n-5)}\mathfrak{S}'L_3 \\ & + \tfrac{1}{2}(n-3)\mathfrak{S}^{\frac{1}{2}(n-5)}\mathfrak{S}^{\cdot}L_4 + \tfrac{1}{2}(n-3)\tfrac{1}{2}(n-5)\mathfrak{S}^{\frac{1}{2}(n-7)}\mathfrak{S}^{\cdot 2}L_5 + \tfrac{1}{2}(n-3)\mathfrak{S}^{\frac{1}{2}(n-5)}\mathfrak{S}^{\cdot\cdot}L_5 \\ & + \tfrac{1}{2}(n-3)\tfrac{1}{2}(n-5)\mathfrak{S}^{\frac{1}{2}(n-7)}\mathfrak{S}^{\cdot}\mathfrak{S}'L_6 + \tfrac{1}{2}(n-3)\mathfrak{S}^{\frac{1}{2}(n-5)}\mathfrak{S}'^{\cdot}L_6 + \mathfrak{S}^{\frac{1}{2}(n-3)}L_1] \end{aligned}$$

$$H_2 = \tfrac{1}{2}(n-1)p[(n-3)\tilde{S}^{\frac{1}{2}(n-5)}\tilde{S}'L_2 + \tilde{S}^{\frac{1}{2}(n-3)}L_3 + \tfrac{1}{2}(n-3)\tilde{S}^{\frac{1}{2}(n-5)}\tilde{S}^{\cdot}L_6]$$

$$H_3 = \tfrac{1}{2}(n-1)p\tilde{S}^{\frac{1}{2}(n-3)}L_2$$

$$H_4 = \tfrac{1}{2}(n-1)p[\tilde{S}^{\frac{1}{2}(n-3)}L_4 + (n-3)\tilde{S}^{\frac{1}{2}(n-5)}\tilde{S}^{\cdot}L_5 + \tfrac{1}{2}(n-3)\tilde{S}^{\frac{1}{2}(n-5)}\tilde{S}'L_6]$$

$$H_5 = \tfrac{1}{2}(n-1)p\tilde{S}^{\frac{1}{2}(n-3)}L_5$$

$$H_6 = \tfrac{1}{2}(n-1)p\tilde{S}^{\frac{1}{2}(n-3)}L_6$$

for λ infinite

$$H_1 = 2\tilde{S}L_1 + \tfrac{1}{2}(n-1)(\tilde{S}''L_2 + \tilde{S}'L_3 + \tilde{S}^{\cdot}L_4 + \tilde{S}^{\cdot\cdot}L_5 + \tilde{S}'^{\cdot}L_6)$$

$$H_2 = \tfrac{1}{2}(n-1)[(n-3)\tilde{S}'L_2 + \tilde{S}L_3 + \tfrac{1}{2}(n-3)\tilde{S}^{\cdot}L_6]$$

$$H_3 = \tfrac{1}{2}(n-1)\tilde{S}L_2$$

$$H_4 = \tfrac{1}{2}(n-1)[\tilde{S}L_4 + (n-3)\tilde{S}^{\cdot}L_5 + \tfrac{1}{2}(n-3)\tilde{S}'L_6]$$

$$H_5 = \tfrac{1}{2}(n-1)\tilde{S}L_5$$

$$H_6 = \tfrac{1}{2}(n-1)\tilde{S}L_6.$$

(b) *Plane strain (λ infinite).* The A's in equation (2.13) are

$$A_{4m} = c_1 x^4 \sin m\theta$$

$$A_{3m} = 2x^3(c_1 + xc_3)\sin m\theta$$

$$A_{2m} = x^2[\{-c_1(1+2m^2) + x^2c_2 + xc_3 - c_5\}\sin m\theta + 2mc_4 \cos m\theta]$$

$$A_{1m} = x[\{c_1(1+2m^2) - x^2c_2 - xc_3(1+2m^2) + c_5\}\sin\theta + m(4xc_6 - 2c_4)\cos m\theta]$$

$$A_{0m} = [c_1(m^4 - 4m^2) + x^2c_2m^2 + 3xc_3m^2 - c_5m^2]\sin m\theta + [c_4(4m - 2m^3) - 4xc_6m]\cos m\theta$$

where

$$c_1 = \tilde{S}^2$$

$$c_2 = \tfrac{1}{2}(n-1)[\tfrac{1}{2}(n-3)\tilde{S}'^2 + \tilde{S}\tilde{S}'']$$

$$c_3 = \tfrac{1}{2}(n-1)\tilde{S}\tilde{S}'$$

$$c_4 = \tfrac{1}{2}(n-1)\tilde{S}\tilde{S}^{\cdot}$$

$$c_5 = \tfrac{1}{2}(n-1)[\tfrac{1}{2}(n-3)\tilde{S}^{\cdot 2} + \tilde{S}\tilde{S}^{\cdot\cdot}]$$

$$c_6 = \tfrac{1}{2}(n-1)[\tfrac{1}{2}(n-3)\tilde{S}^{\cdot}\tilde{S}' + \tilde{S}\tilde{S}'^{\cdot}].$$

The d's in equation (2.17) are

$$d_1 = c_1x^4 + H_3Sx^2$$

$$d_2 = 2c_1x^3 + 2c_3x^4 + H_2Sx^2 + 3H_3Sx + 2H_3S'x^2 + H_6S^{\cdot}x^2$$

$$d_3 = 2H_3S_{r\theta}x + H_6Sx^2$$

$$d_4 = -c_1x^2 + c_2x^4 + c_3x^3 - c_5x^2 + H_1Sx^2 + H_2Sx + H_2S'x^2 + H_3S''x^2 + 2H_3S'x + H_4S^{\cdot}x^2 + H_5S^{\cdot\cdot}x^2 + H_6S'^{\cdot}x^2 + H_6S^{\cdot}x$$

$$d_5 = 2c_4x^2+2H_2S_{r\theta}x+2H_3S_{r\theta}+4H_3S'_{r\theta}x+H_4Sx^2+2H_5S^{\cdot}x^2+H_6Sx+2H_6S^{\cdot}_{r\theta}x+H_6S'x^2$$

$$d_6 = 2c_1x^2-H_3S+H_5Sx^2+2H_6S_{r\theta}x$$

$$d_7 = c_1x-c_2x^3-c_3x^2+c_5x-H_1xS-H_2S-H_2S'x-H_3S''x-2H_3S'$$
$$-H_4S^{\cdot}x-H_5S^{\cdot\cdot}x-H_6S''x-H_6S^{\cdot}$$

$$d_8 = -2c_4x+4c_6x^2+2H_1S_{r\theta}x+2H_2S'_{r\theta}x+2H_3S''_{r\theta}x-H_4Sx+2H_4S^{\cdot}_{r\theta}x$$
$$+2H_5S^{\cdot\cdot}_{r\theta}x-2H_5S^{\cdot}x-H_6S+2H_6S''_{r\theta}x-H_6S'x$$

$$d_9 = -2c_1x+2c_3x^2-H_2S-2H_3S'+2H_4S_{r\theta}x-H_5Sx+4H_5S^{\cdot}_{r\theta}x-H_6S^{\cdot}+2H_6S'_{r\theta}x$$

$$d_{10} = 2H_5S_{r\theta}x-H_6S$$

$$d_{11} = 0$$

$$d_{12} = 4c_4-4c_6x-2H_1S_{r\theta}-2H_2S'_{r\theta}-2H_3S''_{r\theta}-2H_4S^{\cdot}_{r\theta}-2H_5S^{\cdot\cdot}_{r\theta}-2H_6S''_{r\theta}$$

$$d_{13} = 4c_1-c_2x^2-3c_3x+c_5-H_1S-H_2S'-H_3S''-2H_4S_{r\theta}$$
$$-H_4S^{\cdot}-H_5S^{\cdot\cdot}-4H_5S^{\cdot}_{r\theta}-H_6S''-2H_6S'_{r\theta}$$

$$d_{14} = 2c_4-H_4S-2H_5S_{r\theta}-2H_5S^{\cdot}-H_6S'$$

$$d_{15} = c_1-H_5S$$

where

$$S = \tfrac{1}{2}(S_\theta-S_r)$$

$$H_1 = 2\tilde{S}L_1+\tfrac{1}{2}(n-1)(\tilde{S}''L_2+\tilde{S}'L_3+\tilde{S}^{\cdot}L_4+\tilde{S}^{\cdot\cdot}L_5+\tilde{S}''L_6)$$

$$H_2 = \tfrac{1}{2}(n-1)[(n-3)\tilde{S}'L_2+\tilde{S}L_3+\tfrac{1}{2}(n-3)\tilde{S}^{\cdot}L_6]$$

$$H_3 = \tfrac{1}{2}(n-1)\tilde{S}L_2$$

$$H_4 = \tfrac{1}{2}(n-1)[\tilde{S}L_4+(n-3)\tilde{S}^{\cdot}L_5+\tfrac{1}{2}(n-3)\tilde{S}'L_6]$$

$$H_5 = \tfrac{1}{2}(n-1)\tilde{S}L_5$$

$$H_6 = \tfrac{1}{2}(n-1)\tilde{S}L_6$$

and

$$L_1 = x^4F''''+2x^3F'''-x^2F''+2x^2F''^{\cdot}+xF'-2xF'^{\cdot}+4F^{\cdot\cdot}+F^{\cdot\cdot\cdot\cdot}$$

$$L_2 = x^4F''-x^3F'-x^2F^{\cdot\cdot}$$

$$L_3 = 2x^4F'''+x^3F''-x^2F'+2x^2F'^{\cdot}-3xF^{\cdot\cdot}$$

$$L_4 = 2x^2F''^{\cdot}-2xF^{\cdot\cdot}+2F^{\cdot\cdot\cdot}+4F^{\cdot}$$

$$L_5 = F^{\cdot\cdot}+xF'-x^2F''$$

$$L_6 = 4(x^2F^{\cdot\cdot}-xF^{\cdot}).$$

APPENDIX C

Derivation by Stowell's method of stress concentration factor at a circular hole in an infinite plate under pure shear

Assume that the stress field in an infinite plate with a circular hole under pure shear is

$$\begin{aligned}\sigma_r &= G\sigma_\infty\left(1-\frac{4a^2}{r^2}+\frac{3a^4}{r^4}\right)\sin 2\theta\\ \sigma_\theta &= -G\sigma_\infty\left(1+\frac{3a^4}{r^4}\right)\sin 2\theta\\ \sigma_{r\theta} &= G\sigma_\infty\left(1+\frac{2a^2}{r^2}-\frac{3a^4}{r^4}\right)\cos 2\theta\end{aligned} \tag{C1}$$

where G is a function of $E_s/(E_s)_\infty$. Here E_s is the secant modulus at any point and $(E_s)_\infty$ is the secant modulus at infinity. For the elastic case, E_s is constant everywhere and (C1) gives the elastic solution when $G = 1$, therefore $G(1) = 1$. On the other hand, for the material getting very plastic the stress concentration factor defined as $[(\hat{\sigma})_{a,\pi/4}]/\hat{\sigma}_\infty$ must reduce to unity, hence $G(0) = \sqrt{(3)}/4$ when $[(E_s)_{a,\pi/4}]/(E_s)_\infty \to 0$. This stress field satisfies the boundary conditions both at the hole and at infinity.

Now the equilibrium equations are

$$\begin{aligned}\sigma_r' + r^{-1}\sigma_{r\theta}^{\cdot} + r^{-1}(\sigma_r - \sigma_\theta) &= 0\\ r^{-1}\sigma_\theta^{\cdot} + \sigma_{r\theta}' + 2r^{-1}\sigma_{r\theta} &= 0.\end{aligned}$$

When the assumed stresses are substituted into these equations, the results are

$$\begin{aligned}\sigma_r' + r^{-1}\sigma_{r\theta}^{\cdot} + r^{-1}(\sigma_r - \sigma_\theta) = \sigma_\infty\Bigg[&\left(1-\frac{4a^2}{r^2}+\frac{3a^4}{r^4}\right)\sin 2\theta\left(\frac{E_s}{(E_s)_\infty}\right)'\\ &+r^{-1}\left(1+\frac{2a^2}{r^2}-\frac{3a^4}{r^4}\right)\cos 2\theta\left(\frac{E_s}{(E_s)_\infty}\right)^{\cdot}\Bigg]\frac{dG}{d[E_s/(E_s)_\infty]}\\ r^{-1}\sigma_\theta^{\cdot} + \sigma_{r\theta}' + 2r^{-1}\sigma_{r\theta} = \sigma_\infty\Bigg[&-r^{-1}\left(1+\frac{3a^4}{r^4}\right)\sin 2\theta\left(\frac{E_s}{(E_s)_\infty}\right)^{\cdot}\\ &+\left(1+\frac{2a^2}{r^2}-\frac{3a^4}{r^4}\right)\cos 2\theta\left(\frac{E_s}{(E_s)_\infty}\right)'\Bigg]\frac{dG}{d[E_s/(E_s)_\infty]}.\end{aligned}$$

According to Stowell's arguments, the error in the satisfaction of these equations is proportional to

$$\frac{dG}{d[E_s/(E_s)_\infty]}$$

and it is desired that the mean square of the error be made a minimum; that is

$$\int_0^1\left[\frac{dG}{d[E_s/(E_s)_\infty]}\right]^2 d\frac{E_s}{(E_s)_\infty}$$

should be a minimum. The calculus of variations for this expression gives the Euler equation as

$$-\frac{\mathrm{d}}{\mathrm{d}[E_s/(E_s)_\infty]}\left[2\frac{\mathrm{d}G}{\mathrm{d}[E_s/(E_s)_\infty]}\right]=0$$

and from which

$$G=c_1\frac{E_s}{(E_s)_\infty}+c_2.$$

Here c_1 and c_2 are constant, which can be determined by the conditions $G(1)=1$ and $G(0)=\sqrt{(3)}/4$. Hence

$$G=\left(1-\frac{\sqrt{3}}{4}\right)\frac{E_s}{(E_s)_\infty}+\frac{\sqrt{3}}{4}$$

and the stress concentration factor is

$$\hat{K}=\frac{(\hat{\sigma})_{a,\pi/4}}{\hat{\sigma}_\infty}=1+\left(\frac{4}{\sqrt{3}}-1\right)\frac{(E_s)_{a,\pi/4}}{(E_s)_\infty}.$$

(*Received* 2 *February* 1971; *revised* 1 *July* 1971)

Абстракт—Методом, заключающим ряды фурье и конечные разницы, решаются задачи нелинейных краевых условий бесконечно упруго-пластичной пластинки с круглым отверстием, подверженной действию чистого растяжения и чистого сдвига в бесконечности. На основе этих решений, исследуется важность зависимости Нейбера, между факторами концентрации напряжений и деформации, для задач в плоском напряженном состоянии. Предпологается обобщенная формула Столелма для фактора концентраций напряжений в задачах, в которых птиложенная нагрузка может быть как чистым сдвигом, так и чистым растяжениеи, или далее, другими состояниями напряжений. Путем этого же самого метода, получаются распределения напряжении вокруг жесткого, круглого, цилиндрического включения, находящегося в бесконечной, жестко-пластической матрице, подверженной равномерному сдвигу и растяжению.